

Rényi entropies of generic thermodynamic macrostates in integrable systems

Márton Mestyán¹, Vincenzo Alba¹, and Pasquale Calabrese^{1,2}

¹*SISSA & INFN, via Bonomea 265, 34136 Trieste, Italy and*

²*International Centre for Theoretical Physics (ICTP), 34151, Trieste, Italy*

We study the behaviour of Rényi entropies in a generic thermodynamic macrostate of an integrable model. In the standard quench action approach to quench dynamics, the Rényi entropies may be derived from the overlaps of the initial state with Bethe eigenstates. These overlaps fix the driving term in the thermodynamic Bethe ansatz (TBA) formalism. We show that this driving term can be also reconstructed starting from the macrostate's particle densities. We then compute explicitly the stationary Rényi entropies after the quench from the dimer and the tilted Néel state in XXZ spin chains. For the former state we employ the overlap TBA approach, while for the latter we reconstruct the driving terms from the macrostate. We discuss in full details the limits that can be analytically handled and we use numerical simulations to check our results against the large time limit of the entanglement entropies.

I. INTRODUCTION

The time evolution of the entanglement entropy plays a crucial role in the understanding of the non-equilibrium dynamics of isolated quantum systems, in particular for quantum quenches in many body systems. Indeed, the growth of the entanglement entropy in time has been related to the efficiency of tensor network algorithms [1–4] such as the time dependent density matrix renormalisation group (tDMRG). Furthermore, the extensive value (in subsystem size) reached by the entanglement entropy at long time has been understood as the thermodynamic entropy of the ensemble describing stationary local properties of the system [5–12] and related to other thermodynamic entropy definitions [6, 13–21].

In a quantum quench [22–25], a many-body system is initially prepared in a low-entanglement state $|\Psi_0\rangle$ and is let evolve with a many-body Hamiltonian H such that $[H, |\Psi_0\rangle\langle\Psi_0|] \neq 0$. In this protocol, the entire system is in a pure state at any time, but the reduced density matrix of an arbitrary finite compact subsystem attains a long time limit that can be described by a statistical ensemble (see, e.g., Ref. [25]). Thus, at asymptotically long times, all *local* physical observables relax to stationary values. The properties of the reduced density matrix are captured by a Gibbs (thermal) ensemble for generic systems [26–31] and by a generalised Gibbs ensemble (GGE) for integrable systems [32–60].

In one-dimensional systems, the entanglement entropy after a global quantum quench has been found [8–10, 61–83] to generically grow linearly in time up to a point (linear in subsystem size) when a saturation regime to an extensive value takes place. This time evolution of the von Neumann entanglement entropy for a generic integrable system may be fully understood in terms of a semiclassical quasiparticle picture [61] for the spreading of the entanglement, complemented with the Bethe ansatz knowledge of the stationary state, as shown in [8]. These ideas have been first developed for the time evolution after a quantum quench in integrable models [8], but later they have been generalised to other situations as, e.g., in Refs. [84–90]. However, in spite of its great success, this approach hardly generalises to other entanglement estimators and in particular to the Rényi entanglement entropies defined as

$$S^{(\alpha)}[\rho_A] \equiv \frac{1}{1-\alpha} \ln \text{Tr} \rho_A^\alpha, \quad (\text{I.1})$$

in terms of the RDM ρ_A of the considered subsystem A . The Rényi entropies are very important physical quantities for several reasons. First, their knowledge for different values of the index α gives access to the entire spectrum of the density matrix (see e.g. [91]). Since in the limit $\alpha \rightarrow 1$ one has $S^{(\alpha)}[\rho_A] \rightarrow S[\rho_A] \equiv -\text{Tr} \rho_A \ln \rho_A$, they represent the essence of the replica approach to the entanglement entropy [92]. While the replica method was originally introduced as a theoretical analytic tool to deal with the complexity of ρ_A [92], it has become a fundamental concept to access the entanglement entropy in numerical approaches based on Monte Carlo simulations [93] and also in real experiments [94, 95]: Rényi entanglement entropies (for $\alpha = 2$) have been measured experimentally with cold atoms, both in equilibrium [96] and after a quantum quench [11]. Unfortunately, only for non-interacting systems we know how to generalise the quasiparticle picture for the spreading of the entanglement to the Rényi entropies (see, e.g., [78, 97]). For interacting integrable models, the Thermodynamic Bethe Ansatz (TBA) approach to quantum quenches (overlap TBA or Quench Action method [98, 99]) has been adapted in [97] to the calculation of the stationary value of the Rényi entropies for both the diagonal and GGE ensembles. Within this approach, in the thermodynamic limit, $S^{(\alpha)}$ is given as a generalised free energy over a saddle point eigenstate (representative eigenstate or thermodynamic macrostate) which is *not* the one corresponding to the stationary state describing local observables and von Neumann entropy, as

we shall review later. It turns out that this shifting of the saddle point is the main obstacle toward a quantitative semiclassical formula for the time evolution of the Rényi entanglement entropies whose large time limit is provided by the GGE value.

This general approach, so far has been used for the calculation of the Rényi entropies only for the quench from the Néel state in the XXZ spin-chain [97, 100], finding a very interesting α and Δ dependence. The goal of this manuscript is twofold. On the one hand, we will apply the approach of Refs. [97, 100] to the calculation of the stationary Rényi entropies after the quench from other initial states, a problem *per se* of high interest. On the other hand, this approach strongly depends on the knowledge of the overlaps between the initial state and the Bethe states. These are known in many cases, but the GGE can be also constructed in a simpler way from the conservation of all local and quasilocal charges [50, 58]. In particular until very recently, for many initial states (i.e. tilted Néel and tilted ferromagnet) in the quench in XXZ spin-chain, stationary values were known only by means of the latter method [101]. For this reason, we developed a hybrid numerical/analytic method to get exact predictions for the Rényi entropies which does not require an a-priori knowledge of the overlaps and apply it to the prototypical case of tilted Néel states. However, after the completion of our calculations, a manuscript appeared [102] providing a conjecture for the overlaps also in this case. These served as a test of the validity of our method and did not alter the logic of the calculation which was a proof of concepts about the construction of Rényi entropies without knowing the overlaps.

The paper is organised as follows. In Sec. II we introduce the XXZ spin-chain and review its Bethe ansatz solution. In Sec. III we first review the TBA approach for the Rényi entropies [97], work out some major simplifications on the known expressions, and finally we apply this machinery to the quench from the dimer state, working out explicitly a two limits ($\Delta \rightarrow \infty$ and $\alpha \rightarrow \infty$) that can be handled analytically. In Sec. IV we show how to calculate the Rényi entropies for generic macrostates and we apply this machinery to the explicit case of the tilted Néel state, finding several interesting new results. In Sec. V we test, by means of extensive tDMRG simulations, that the thermodynamic Rényi entropies agree with the long time limit of the entanglement entropies. Finally in Sec. VI we summarise our findings and discuss open problems.

II. THE XXZ MODEL AND ITS BETHE ANSATZ SOLUTION

In this work we consider quantum quenches in the spin-1/2 one-dimensional anisotropic Heisenberg model (XXZ spin chain) with Hamiltonian

$$H = \sum_{k=1}^L [\sigma_k^x \sigma_{k+1}^x + \sigma_k^y \sigma_{k+1}^y + \Delta (\sigma_k^z \sigma_{k+1}^z - 1)], \quad (\text{II.1})$$

where $\sigma_j^{x,y,z}$ are the Pauli matrices and Δ is the anisotropy parameter. We focus on the antiferromagnetic gapped phase for $\Delta > 1$. Periodic boundary conditions are imposed by choosing $\sigma_{L+1}^{x,y,z} = \sigma_1^{x,y,z}$. The Hamiltonian of the XXZ chain commutes with the total magnetisation $S_T^z \equiv \sum_i \sigma_i^z / 2$. As a consequence, the eigenstates of (II.1) can be labelled by the value of S_T^z . Due to periodic boundary conditions, the XXZ chain is invariant under one site translations $\sigma_i^\alpha \rightarrow \sigma_{i+1}^\alpha$. This means that $[\mathcal{T}, H] = 0$, where \mathcal{T} is the one-site translation operator.

In the following, we will consider quantum quenches from the Majumdar-Ghosh (dimer) state and from the tilted Néel state. The dimer state is defined as

$$|\text{D}\rangle = \left(\frac{|\uparrow\downarrow\rangle - |\downarrow\uparrow\rangle}{\sqrt{2}} \right)^{\otimes L/2}. \quad (\text{II.2})$$

To take advantage of the translational invariance of the XXZ chain, we will consider the translation invariant version of the dimer state, which is given as

$$|\Psi_0\rangle = \left(\frac{1 + \mathcal{T}}{\sqrt{2}} \right) |\text{D}\rangle, \quad (\text{II.3})$$

where \mathcal{T} is the one-site translation operator. Indeed, the stationary states for the quench from the dimer state (II.2) and from its translational invariant version (II.3) are the same, but the time evolution is clearly different [49].

We also consider quenches from the tilted Néel state defined as

$$|\Psi_0\rangle = [(\cos(\theta/2)|\uparrow\rangle + i \sin(\theta/2)|\downarrow\rangle) \otimes (-i \sin(\theta/2)|\uparrow\rangle + \cos(\theta/2)|\downarrow\rangle)]^{\otimes L/2}. \quad (\text{II.4})$$

Here θ is the tilting angle. The tilted Néel state is obtained by applying the global rotation operator to the translational invariant version of the Néel state $|N\rangle \equiv |\uparrow\downarrow \dots\rangle$ as

$$|\Psi_0\rangle = e^{i\theta/2 \sum_i \sigma_i^y} \left(\frac{|N\rangle + \mathcal{T}|N\rangle}{\sqrt{2}} \right). \quad (\text{II.5})$$

In this work we are interested in the steady-state Rényi entropies after the quenches from (II.3) and (II.4). For the dimer state we proceed using the technique developed in Refs [97, 100], i.e. exploiting the analytic knowledge of the overlaps between the state and the eigenstates of the XXZ chain. By using the Quench Action method [98, 99] this provides a set of driving functions for a generalised set of TBA equations that determine the steady-state Rényi entropies. Conversely, when we started this work, the overlaps between the tilted Néel state and the eigenstates of the XXZ chain were not known (see Ref. [102] for a recent conjecture). Thus we provide a suitable generalisation of the method of Ref. [97] to reconstruct the driving terms from the stationary ensemble. This generalisation is one of the main technical results of the paper.

A. Bethe ansatz solution of the XXZ chain

The XXZ chain can be solved by the Bethe ansatz [103], which allows one to construct *all* the eigenstates of (II.1) analytically. It is convenient to work in the sector with fixed magnetisation S_T^z , or, equivalently with fixed number N of down spins. Here we follow the standard Bethe ansatz framework referring to down spins as particles. The eigenstates of the XXZ chain are easily constructed starting from the ferromagnetic state, i.e., the state with all the spins up $|\uparrow\uparrow\cdots\rangle$. The Bethe ansatz expression for the generic eigenstate in the sector with N down spins reads

$$|\boldsymbol{\lambda}\rangle = \sum_{n_1 < n_2 < \cdots < n_N} \psi(n_1, n_2, \dots, n_N) \sigma_{n_1}^- \sigma_{n_2}^- \cdots \sigma_{n_N}^- |\uparrow\uparrow\cdots\rangle, \quad (\text{II.6})$$

where σ_i^- is the spin-1/2 lowering operator. Here the sum is over the positions n_i of the particles. The amplitudes $\psi(n_1, n_2, \dots, n_N)$ read

$$\psi(n_1, n_2, \dots, n_N) = \sum_P A(P) \prod_{j=1}^N \left(\frac{\sin(\lambda_{P_j} + i\eta/2)}{\sin(\lambda_{P_j} - i\eta/2)} \right)^{n_j}, \quad (\text{II.7})$$

where $\eta \equiv \text{arcosh}(\Delta)$, and the sum is now over the permutations P of the indices $j \in [1, N]$. The overall amplitude $A(P)$ is given as

$$A(P) = (-1)^{\text{sign}(P)} \prod_{j=1}^N \prod_{k=j+1}^N \sin(\lambda_{P_j} - \lambda_{P_k} + i\eta). \quad (\text{II.8})$$

The state is then specified by a set of N rapidities λ_j that play the same role of the quasimomenta in free models. The total energy of the eigenstate is obtained by summing independently the contributions of each particle, to obtain

$$E = \sum_{j=1}^N e(\lambda_j), \quad e(\lambda) \equiv -\frac{4 \sinh(\eta)^2}{\cosh(\eta) - \cos(2\lambda_j)}. \quad (\text{II.9})$$

In order for (II.6) to be an eigenstate of the XXZ chain, the rapidities have to be solutions of the Bethe equations [103]

$$\left(\frac{\lambda_j + i\eta/2}{\lambda_j - i\eta/2} \right)^L = - \prod_{k=1}^N \frac{\lambda_j - \lambda_k + i\eta}{\lambda_j - \lambda_k - i\eta} \quad (j = 1, \dots, N). \quad (\text{II.10})$$

Each independent set of solutions $\{\lambda_j\}_{j=1}^N$ identifies a different eigenstate of the XXZ chain.

A distinctive property of the XXZ model, which underlies its integrability, is the existence of an infinite number of pairwise commuting *local* and *quasilocal* conserved quantities (charges) [104]

$$Q_s^{(j)} = \left. \frac{d^{j-1}}{d\lambda^{j-1}} T_s(\lambda) \right|_{\lambda=0}, \quad [Q_r^{(j)}, Q_s^{(k)}] = 0, \quad Q_{1/2}^{(2)} = \frac{1}{2 \sinh \eta} H_{\text{XXZ}}. \quad (\text{II.11})$$

Here $T_s(\lambda)$ is the transfer matrix of the XXZ model with an s -dimensional auxiliary space. The dimension s of the auxiliary space can be any positive integer or half-integer. In fact, choosing $s = 1/2$ yields the usual transfer matrix of the six-vertex model [105]. The corresponding charges $Q_{1/2}^{(j)}$ are local, which means they are of the sum of operators that act non-trivially at most at $m^{(j)}$ sites, where $m^{(j)}$ is an integer depending on j . For example, the charge $Q_{1/2}^{(2)}$ has $m^{(2)} = 2$ and it is proportional to the system Hamiltonian (II.1). On the other hand, there is no such limit on the

size of the terms in the charges $Q_s^{(j)}$ when $s > 1/2$. These charges, called *quasilocal charges*, are crucial to correctly describe the steady state arising after a quantum quench in integrable models [50].

Since the charges (II.11) commute with the Hamiltonian (II.1), all of them are diagonal in the basis of Bethe ansatz eigenstates (II.6)-(II.10). The corresponding eigenvalues are given as [104]

$$Q_s^{(j)}|\boldsymbol{\lambda}\rangle = \sum_{k=1}^N q_s^{(j)}(\lambda_k)|\boldsymbol{\lambda}\rangle + o(L), \quad q_s^{(j)}(\lambda) = \left(-i \frac{d}{d\mu}\right)^{j-1} \ln \left(\frac{\sin(\mu - \lambda + is\eta)}{\sin(\mu - \lambda - is\eta)}\right) \Big|_{\mu=0}, \quad (\text{II.12})$$

where $o(L)$ indicates terms that are either zero (in the case of local charges with $s = 1/2$) or vanish in the thermodynamic limit (in the case of quasilocal charges with $s > 1/2$).

B. Thermodynamic Bethe Ansatz (TBA)

In this paper we are interested in the thermodynamic limit $L, N \rightarrow \infty$, with the ratio N/L (i.e., the particle density) fixed. The solutions of the Bethe equations (II.10) are in general complex. However, a remarkable feature of the Bethe equations is that in the thermodynamic limit their solutions are organised into strings, i.e., multiplets of solutions having the same real part, but different imaginary components. This is the famous string hypothesis [103]. Precisely, the generic structure of a string multiplet reads

$$\lambda_{n,j}^\alpha = \lambda_n^\alpha + \frac{i\eta}{2}(n+1-2j) + \delta_{n,j}^\alpha. \quad (\text{II.13})$$

Here n is the string length, i.e., the number of solutions with the same real part, α labels the different strings of the same size n , and j labels the different components within the same string multiplet. The *real* number λ_n^α is called string center. The string hypothesis holds only in the thermodynamic limit: for finite chains, string deviations (denoted as $\delta_{n,j}^\alpha$ in (II.13)) are present, but for thermodynamically relevant states, they vanish exponentially in L .

In the thermodynamic limit the string centers become dense on the real axis. Thus, instead of working with individual eigenstates, it is convenient to describe the thermodynamic quantities by introducing the densities $\rho_n(\lambda)$, one for each string type n . $\rho_n(\lambda)$ are the densities of string centers on the real line. Similarly, one can introduce the densities of holes $\rho_{h,n}(\lambda)$, which is the density of unoccupied string centers, and the total density (density of states) $\rho_{t,n}(\lambda) \equiv \rho_n(\lambda) + \rho_{h,n}(\lambda)$. Each set of particle and hole densities identify a thermodynamic macrostate of the XXZ chain. Moreover, a given set of densities $\rho_n(\lambda)$ corresponds to an exponentially large (with L and N) number of microscopic eigenstates. The rapidities identifying all these eigenstates converge in the thermodynamic limit to the same set of densities. The logarithm of the number of thermodynamically equivalent eigenstates is given by the Yang–Yang entropy [106]

$$S_{YY} = s_{YY}L = L \sum_{n=1}^{\infty} \int d\lambda [\rho_{t,n}(\lambda) \ln \rho_{t,n}(\lambda) - \rho_n(\lambda) \ln \rho_n(\lambda) - \rho_{h,n}(\lambda) \ln \rho_{h,n}(\lambda)]. \quad (\text{II.14})$$

The Yang–Yang entropy is extensive, and its density is obtained by summing independently the contributions of the different rapidities and string types n . The only constraint that a legitimate set of densities has to satisfy is given by the continuum limit of the Bethe equations, which are called Bethe–Gaudin–Takahashi (BGT) equations [103]

$$\rho_{t,n} = a_n - \sum_{m=1}^{\infty} A_{nm} \star \rho_m, \quad (\text{II.15})$$

where we defined

$$a_n(\lambda) \equiv \frac{1}{\pi} \frac{\sinh(n\eta)}{\cosh(n\eta) - \cos(2\lambda)}. \quad (\text{II.16})$$

In (II.15), A_{nm} are the scattering phases between the bound states, defined as

$$A_{nm}(\lambda) \equiv (1 - \delta_{n,m})a_{|n-m|}(\lambda) + a_{|n-m|+2}(\lambda) + \cdots + a_{n+m-2}(\lambda) + a_{n+m}(\lambda), \quad (\text{II.17})$$

and the star symbol \star denotes the convolution

$$[f \star g](\lambda) \equiv \int_{-\pi/2}^{\pi/2} d\mu f(\lambda - \mu)g(\mu). \quad (\text{II.18})$$

Importantly, a standard trick in Bethe ansatz allows one to simplify (II.15) obtaining a system of partially decoupled integral equations as [103]

$$\rho_{t,n} = s \star (\rho_{h,n-1} + \rho_{h,n+1}) \quad (n = 1, 2, \dots), \quad (\text{II.19})$$

where, for the sake of simplicity, we defined $\rho_{h,0}(\lambda) \equiv \delta(\lambda)$, and we introduced $s(\lambda)$ as

$$s(\lambda) \equiv \frac{1}{2\pi} \sum_{k=-\infty}^{\infty} \frac{e^{-2ik\lambda}}{\cosh k\eta} = \frac{1}{2\pi} + \frac{1}{2\pi} \sum_{k=1}^{\infty} \frac{\cos 2k\lambda}{\cosh k\eta}. \quad (\text{II.20})$$

The partially decoupled system is typically easier to solve numerically than (II.15).

In the thermodynamic limit, the eigenvalues of the conserved quantities $Q_s^{(j)}$ (II.12) can be written in terms of the densities ρ_n as

$$\langle \rho | Q_s^{(j)} | \rho \rangle = \sum_{n=1}^{\infty} \int_{-\pi/2}^{\pi/2} d\lambda \rho_n(\lambda) q_{s,n}^{(j)}(\lambda), \quad q_{s,n}^{(j)} = \sum_{k=1}^n q_s^{(j)} \left(\lambda + \frac{i\eta}{2} (n+1-2k) \right). \quad (\text{II.21})$$

Here $q_s^{(j)}$ is the same as in (II.12).

III. TBA APPROACH FOR THE STATIONARY RÉNYI ENTROPIES

In this section we summarise the recently developed TBA approach to compute Rényi entropies in the steady state at long time after a quantum quench [97, 100]. In integrable models, the steady-state can be characterised in terms of the initial-state expectation value of the infinite set of local and quasilocal conserved charges (II.11). These conserved quantities are key to construct the GGE that describes local and quasilocal observables in the steady state. The density matrix of the GGE is

$$\rho_{\text{GGE}} \equiv \frac{1}{Z_{\text{GGE}}} \exp \left(- \sum_{s,j} \beta_s^{(j)} Q_s^{(j)} \right), \quad Z_{\text{GGE}} \equiv \text{Tr} \exp \left(- \sum_{s,j} \beta_s^{(j)} Q_s^{(j)} \right), \quad (\text{III.1})$$

where $Q_s^{(j)}$ are the local and quasilocal conserved charges ($s = 1/2, 1, 3/2, 2, \dots$ and $j = 1, 2, \dots$), and Z_{GGE} is a normalisation. The Lagrange multipliers $\beta_s^{(j)}$ fix the GGE expectation values of the charges to their initial-state values $\langle \Psi_0 | Q_s^{(j)} | \Psi_0 \rangle$. Similarly to the standard (thermal) TBA, local and quasilocal properties of the steady state are fully encoded in an appropriate thermodynamic macrostate [98, 99], which is fully characterised by a set of densities ρ_n and $\rho_{h,n}$.

The GGE Rényi entropies are by definition

$$S_{\text{GGE}}^{(\alpha)} = \frac{1}{1-\alpha} \ln \text{Tr} \rho_{\text{GGE}}^\alpha. \quad (\text{III.2})$$

After plugging (III.1) into (III.2), the Renyi entropies read

$$S_{\text{GGE}}^{(\alpha)} = \frac{1}{1-\alpha} \left[\ln \text{Tr} \exp \left(-\alpha \sum_{s,j} \beta_s^{(j)} Q_s^{(j)} \right) - \alpha \ln Z_{\text{GGE}} \right]. \quad (\text{III.3})$$

We now review the TBA approach to calculate the GGE Rényi entropies. First, the trace over the eigenstates in (III.3) in the thermodynamic limit is replaced by a functional integral over the TBA densities ρ_n as

$$\text{Tr} \rightarrow \int D[\rho] e^{S_{\text{YY}}}, \quad (\text{III.4})$$

where we defined $D[\rho] \equiv \prod_n D\rho_n(\lambda)$. In Eq. (III.4) the Yang-Yang entropy takes into account that there is an exponentially large (with system size) number of microscopic eigenstates corresponding to the same thermodynamic state. The Rényi entropies (III.3) are then given by the functional integral [97, 100]

$$S_{\text{GGE}}^{(\alpha)} = \frac{1}{1-\alpha} \left[\ln \int D[\rho] \exp(-\alpha \mathcal{E}[\rho] + S_{\text{YY}}[\rho]) + \alpha f_{\text{GGE}} \right]. \quad (\text{III.5})$$

Here we introduce the pseudoenergy $\mathcal{E}[\rho]$ as

$$\mathcal{E}[\rho] \equiv \sum_{s,j} \beta_s^{(j)} Q_s^{(j)}[\rho] = L \sum_{s,j} \beta_s^{(j)} \sum_n \int d\lambda \rho_n(\lambda) q_{s,n}^{(j)}(\lambda), \quad (\text{III.6})$$

where $q_{s,n}^{(j)}$ are defined in (II.21). (In the case of the standard Gibbs ensemble the sum includes only the energy $q_{1/2,n}^{(2)}(\lambda)$ coupled with the inverse temperature $\beta_{1/2}^{(2)}$.) The quantity f_{GGE} is the GGE grand canonical potential defined as

$$f_{\text{GGE}} = -\ln Z_{\text{GGE}}. \quad (\text{III.7})$$

Following the standard TBA treatment [103], the functional integral in (III.5) can be evaluated using the saddle-point method [97, 100] because both S_{YY} and \mathcal{E} are extensive. Formally, this corresponds to minimising with respect to ρ_n the functional $\mathcal{S}_{\text{GGE}}^{(\alpha)}$ defined as

$$\mathcal{S}_{\text{GGE}}^{(\alpha)}[\rho] \equiv -\alpha \mathcal{E}[\rho] + S_{\text{YY}}[\rho]. \quad (\text{III.8})$$

Notice in (III.8) the explicit dependence on the Rényi index α . For $\alpha = 1$, Eq. (III.8) provides the macrostate that describes local and quasilocal properties of the steady state [98, 99] and the von Neumann entropy [8]. The minimisation procedure gives a set of coupled integral equations for the macrostate densities $\rho_n^{(\alpha)}$. These are conveniently written in terms of a set of functions $\eta_n^{(\alpha)}(\lambda) = \rho_{h,n}^{(\alpha)}(\lambda)/\rho_n^{(\alpha)}(\lambda)$, where α is the index of the Rényi entropy. Specifically, the saddle point condition on (III.8) yields the equations

$$\ln \eta_n^{(\alpha)} = \alpha g_n + \sum_{m=1}^{\infty} A_{nm} \star \ln[1 + 1/\eta_m^{(\alpha)}], \quad (\text{III.9})$$

where $A_{nm}(\lambda)$ is defined in (II.17), and the TBA driving function $g_n(\lambda)$ is defined as

$$g_n(\lambda) \equiv \sum_{s,j} \beta_s^{(j)} q_{s,n}^{(j)}(\lambda). \quad (\text{III.10})$$

Here $q_{s,n}^{(j)}(\lambda)$ are the functions expressing the eigenvalues of (quasi)local charges as in (II.21). Similarly to the standard TBA [103], it is possible to partially decouple the system of integral equations (III.9), obtaining

$$\ln \eta_n^{(\alpha)} = \alpha d_n + s \star \ln(1 + \eta_{n-1}^{(\alpha)})(1 + \eta_{n+1}^{(\alpha)}) \quad (\eta_0 \equiv 0), \quad (\text{III.11})$$

with the source terms d_n being defined as

$$d_n = g_n - s \star (g_{n-1} + g_{n+1}) \quad (g_0 \equiv 0). \quad (\text{III.12})$$

This set of equations is easier to solve numerically than (III.9) because they contain fewer convolutions. Once the solutions $\eta_n^{(\alpha)}(\lambda)$ are determined, the particle densities $\rho_n^{(\alpha)}$ are obtained by using the thermodynamic Bethe equations (II.19). Finally, the GGE Rényi entropy (III.3) is obtained by evaluating (III.5) on the densities $\rho_n^{(\alpha)}$ as

$$\mathcal{S}_{\text{GGE}}^{(\alpha)} = \frac{1}{\alpha - 1} \left[\left(\alpha \mathcal{E} - S_{\text{YY}} \right) \Big|_{\rho_n^{(\alpha)}} + \alpha f_{\text{GGE}} \Big|_{\rho_n^{(1)}} \right], \quad (\text{III.13})$$

where $\mathcal{E}[\rho]$ and $S_{\text{YY}}[\rho]$ are functionals of the string densities defined in (III.6) and (II.14), and f_{GGE} is the grand canonical potential (III.7). Note that f_{GGE} is calculated over the macrostate $\rho_n^{(1)}$, i.e., with $\alpha = 1$; for all the quenches that can be treated with the Quench Action method one has $f_{\text{GGE}} = 0$, due to the normalisation of the overlaps.

Once again, we stress that the thermodynamic macrostate describing the Rényi entropies is not the same as that characterising the local observables, or the von Neumann entropy, and it depends on α . This has the intriguing consequence that different Rényi entropies, in principle, contain information about different regions of the spectrum of the post-quench Hamiltonian. This difference does not come as a surprise when considering the thermodynamic entropies. However, the thermodynamic entropies are the same as the entanglement entropies of a subsystem that is large in itself but a vanishing fraction of the whole system. Therefore the difference is very puzzling because entanglement entropies are all calculated from the same quantum mechanical wavefunction.

A technical remark is now in order. Although the procedure to extract the Rényi entropies that we outlined so far is legitimate, a crucial ingredient is the set of infinitely many Lagrange multipliers $\beta_s^{(j)}$ entering in (III.10) and in the driving functions g_n (cf. (III.10)). In principle, they are fixed by requiring that the GGE averages of the local and quasilocally conserved quantities $Q_s^{(j)}$ equal their expectation values over the initial state. However, this is a formidable task that cannot be carried out in practice. As of now, it is possible to overcome this difficulty in two ways. One is to use the Quench Action method [98, 99], as discussed below. The other way, based on the analytical solution of the GGE saddle point equations, will be described in Section IV. The Quench Action gives access to the thermodynamic macrostate describing local and quasilocally observables (and the thermodynamic entropy) in the stationary state at long times. Crucially, the Quench Action allows one to extract the driving functions g_n without relying on the knowledge of the $\beta_s^{(j)}$. The key ingredients are the overlaps between the initial state and all the eigenstates of the post-quench Hamiltonian, although a subset of the thermodynamically relevant overlaps may be sufficient (see [107–109]). Crucially, for a large class of initial states the overlaps can be calculated analytically [102, 110–124]. Overlap calculations are possible also for systems in the continuum, such as the Lieb-Liniger gas. For example, in Refs. [113–115], the overlaps between the Bose condensate (BEC) state and the eigenstates of the Lieb-Liniger model with both repulsive and attractive interactions, have been calculated and used in [114, 125] to study their dynamics. The information about the driving functions was crucial in Ref. [100] to obtain the steady-state value of the Rényi entropies after the quench from the Néel state. Interestingly, all the initial states for which it has been possible to calculate the overlaps in interacting models are reflection symmetric. The defining property of reflection-symmetric states is that they have nonzero overlap only with parity-invariant eigenstates, which correspond to solutions of the Bethe equations that contain only pairs of rapidities with opposite sign, i.e., such that $\{\lambda_j\}_{j=1}^N = \{-\lambda_j\}_{j=1}^N$. Indeed, the importance of parity-invariance for the solvability of quantum quenches has been explored in Ref. [126] for integrable lattice models and in Ref. [127] for integrable field theories. However, some non reflection symmetric initial states for which the Quench Action method can be applied have been found in the Hubbard chain in the infinite repulsion limit in Ref. [124].

A. A simplified expression for the Rényi entropies

The GGE Rényi entropy as expressed in (III.13) are functionals of an infinite set of densities $\rho_n(\lambda)$. In this section we show that it is possible to simplify (III.13) writing the Rényi entropies only in terms of $\eta_1^{(\alpha)}$. A formula similar to the one we are going to derive is known for the Gibbs (thermal) free energy since many years [103].

The first step in this derivation is to rewrite (III.13) as

$$S_{\text{GGE}}^{(\alpha)} = \frac{L}{\alpha - 1} \sum_{n=1}^{\infty} \int_{-\pi/2}^{\pi/2} d\lambda \left[\alpha \rho_n^{(\alpha)}(\lambda) g_n(\lambda) - \rho_n^{(\alpha)}(\lambda) \ln(1 + \eta_n^{(\alpha)}(\lambda)) - \rho_{h,n}^{(\alpha)}(\lambda) \ln(1 + 1/\eta_n^{(\alpha)}(\lambda)) \right] + \frac{\alpha L}{\alpha - 1} f_{\text{GGE}}. \quad (\text{III.14})$$

The function $\alpha g_n(\lambda)$ can be obtained from Eq. (III.9), whereas $\rho_{h,n}^{(\alpha)}(\lambda)$ can be obtained from the BGT equations in (II.15). After some algebra this yields

$$S_{\text{GGE}}^{(\alpha)} = \frac{L}{1 - \alpha} \left[\sum_{n=1}^{\infty} \int_{-\pi/2}^{\pi/2} d\lambda a_n(\lambda) \ln(1 + 1/\eta_n^{(\alpha)}(\lambda)) - \alpha f_{\text{GGE}} \right]. \quad (\text{III.15})$$

The infinite sum in (III.15) can be further simplified by considering the first of the saddle point equations in (III.9)

$$\ln(1 + \eta_1^{(\alpha)}(\lambda)) = g_1(\lambda) + \sum_{m=1}^{\infty} \int_{-\pi/2}^{\pi/2} d\mu [a_{m-1}(\lambda - \mu) + a_{m+1}(\lambda - \mu)] \ln(1 + 1/\eta_m^{(\alpha)}(\mu)). \quad (\text{III.16})$$

One then has to multiply (III.16) by $s(\lambda)$ (cf. (II.20)) and integrate over λ . Finally, after some manipulations (identical to those appearing in Ref. [107]), one obtains

$$\int_{-\pi/2}^{\pi/2} d\lambda s(\lambda) \left[\ln(1 + \eta_1^{(\alpha)}(\lambda)) - g_1(\lambda) \right] = \sum_{n=1}^{\infty} \int_{-\pi/2}^{\pi/2} d\lambda a_n(\lambda) \ln(1 + 1/\eta_n^{(\alpha)}(\lambda)). \quad (\text{III.17})$$

The right-hand side of (III.17) is precisely the first term in the square brackets in (III.15). Plugging (III.17) into (III.15), one obtains the simplified formula for the Rényi entropy as

$$S_{\text{GGE}}^{(\alpha)} = \frac{L}{\alpha - 1} \left\{ \int_{-\pi/2}^{\pi/2} d\lambda s(\lambda) \left[\alpha g_1(\lambda) - \ln(1 + \eta_1^{(\alpha)}(\lambda)) \right] + \alpha f_{\text{GGE}} \right\}, \quad (\text{III.18})$$

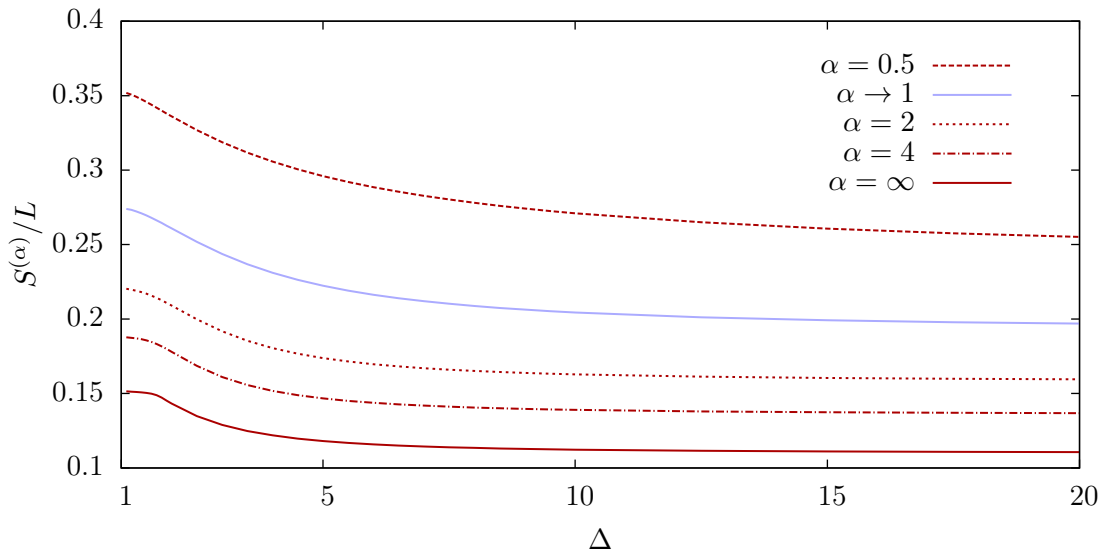


FIG. 1. Rényi entropies of the GGE after the quench from the dimer state in the XXZ chain. The entropy densities $S^{(\alpha)}/L$ are plotted as a function of the chain anisotropy Δ . The different lines denote results for different Rényi index α . In the limit $\Delta \rightarrow \infty$ all the Rényi entropies remain finite.

which is our final result depending only on $\eta_1^{(\alpha)}(\lambda)$.

An important remark is that while (III.18) depends only on one rapidity density, it is still necessary to solve the full set of TBA equations (III.9) in order to determine $\eta_1^{(\alpha)}$, because all the $\eta_n^{(\alpha)}$ are coupled. However, Eq. (III.18) has at least two advantages. First, it is more convenient than (III.13) from the numerical point of view, because it contains less integrals to be evaluated. Second, Eq. (III.18) is more convenient for analytical manipulations.

B. Rényi entropies after quenching from the dimer state

In this section we employ the TBA approach described above to calculate the Rényi entropies after the quench from the dimer state, generalising the results of Ref. [100] for the quench from the Néel state. For the dimer state, the overlaps are analytically known [108, 112] and hence the Quench Action provides the driving functions g_n as [108]

$$g_1(\lambda) = -\ln \left(\frac{\sinh^4(\lambda) \cot^2(\lambda)}{\sin(2\lambda + i\eta) \sin(2\lambda - i\eta)} \right), \quad (\text{III.19})$$

$$g_n(\lambda) = \sum_{k=1}^n g_1(\lambda + i\eta(n+1-2k)/2), \quad (n \geq 2),$$

$$d_n(\lambda) = -\ln \left(\frac{\vartheta_4(\lambda)}{\vartheta_1(\lambda)} \right)^2 + (-1)^n \ln \left(\frac{\vartheta_2(\lambda)}{\vartheta_3(\lambda)} \right)^2, \quad (\text{III.20})$$

where $\vartheta_\ell(x)$ are the Jacobi ϑ -functions with nome $e^{-2\eta}$.

The strategy to calculate the Rényi entropies is to use the driving function g_n in the TBA equations for $\eta_n^{(\alpha)}$ (cf. (III.9)). After solving for $\eta_n^{(\alpha)}$, the GGE Rényi entropies are obtained from (III.18). Obviously, the term f_{GGE} has to be evaluated using the density $\rho_n^{(1)}$ (cf. (III.13)), but normalisation provides $f_{\text{GGE}} = 0$.

The numerical results for the Rényi entropies obtained with this procedure are shown in Figure 1. The Figure shows the entropy densities $S^{(\alpha)}/L$ plotted versus the chain anisotropy Δ . Different lines correspond to different values of α . As expected, one has that for any Δ , $S^{(\alpha)} < S^{(\alpha')}$ if $\alpha > \alpha'$. For completeness we report the result for $\alpha \rightarrow 1$. An interesting observation is that the Rényi entropies do not vanish in the Ising limit for $\Delta \rightarrow \infty$. This is in contrast with what happens for the quench from the Néel state, for which the steady-state entropies at $\Delta \rightarrow \infty$ vanish. The reason is that the Néel state becomes the ground state of the XXZ chain in that limit, and there is no dynamics after the quench. In some limiting cases it is possible to derive closed analytic formulas for the post-quench stationary

Rényi entropy: in the following, we will provide analytical results in the Ising limit $\Delta \rightarrow \infty$ and for the min entropy, i.e., the limit $\alpha \rightarrow \infty$.

C. Expansion of Rényi entropies in the Ising limit

In this section we perform an expansion of the steady-state Rényi entropies in the large Δ limit, by closely following the procedure introduced in [107]. A similar expansion for the Rényi entropies after the quench from the Néel state has been carried out in [97]. In that case, the $\Delta \rightarrow \infty$ limit is very special, since the Néel state becomes the ground state of the model, and there is no dynamics. The quench from the dimer state is more generic, because the dimer state is never an eigenstate of the chain, and consequently the post-quench dynamics is nontrivial, implying that the stationary value of the Rényi entropy is nonzero also for $\Delta \rightarrow \infty$. We anticipate that in the Ising limit the Rényi entropies have the same form as for free-fermion models [97], but deviations from the free-fermion result appear already at the first non trivial order in $1/\Delta$.

In the following we obtain the steady-state Rényi entropies as a power series in the variable $z \equiv e^{-\eta}$ with $\eta = \text{arccosh}(\Delta)$. Following [100], we use the ansatz for $\eta_n^{(\alpha)}$

$$\eta_n^{(\alpha)}(\lambda) = z^{\beta_n(\alpha)} \eta_{n,0}^{(\alpha)}(\lambda) \exp\left(\Phi_n^{(\alpha)}(z, \lambda)\right). \quad (\text{III.21})$$

Here the exponents $\beta_n(\alpha)$, the functions $\Phi_n^{(\alpha)}(\lambda)$, and $\eta_{n,0}^{(\alpha)}$ have to be determined by plugging the ansatz (III.21) into the TBA equations (III.11). We also need the expansion of the driving functions d_n around $z = 0$:

$$d_n = \begin{cases} \ln(4 \sin^2(2\lambda)) z^2 + 4 \cos(4\lambda) z^4 + O(z^6) & n \text{ even,} \\ \ln(\tan^2(\lambda)) + 8 \cos(2\lambda) z^2 - 8 \cos(2\lambda) z^4 + O(z^6) & n \text{ odd.} \end{cases} \quad (\text{III.22})$$

The expansion of the kernel $s(\lambda)$ appearing in (III.11) is

$$s(\lambda) = \frac{1}{2\pi} + \frac{2}{\pi} \cos(2\lambda) z + \frac{2}{\pi} \cos(4\lambda) z^2 + O(z^3). \quad (\text{III.23})$$

After plugging the ansatz (III.21) into (III.11), and considering the leading order in powers of z , one can fix the exponents β_n . By treating separately the cases of even and odd n in (III.22), one finds

$$\beta_n = \begin{cases} 2\alpha & n \text{ even,} \\ 0 & n \text{ odd.} \end{cases} \quad (\text{III.24})$$

This choice is not unique, but it is the only one that is consistent with the BGT equations (II.19), see [107]. The leading order in z of (III.11) fixes the functions $\eta_{n,0}(\lambda)$ as

$$\eta_{n,0}^{(\alpha)}(\lambda) = \begin{cases} 4^\alpha e^{c(\alpha)} |\sin(\lambda)|^{2\alpha} & n \text{ even,} \\ |\tan(\lambda)|^{2\alpha} & n \text{ odd,} \end{cases} \quad (\text{III.25})$$

where the constant $c(\alpha)$ is given as

$$c(\alpha) = \frac{1}{\pi} \int_{-\pi/2}^{\pi/2} d\mu \ln(1 + |\tan(\mu)|^{2\alpha}). \quad (\text{III.26})$$

In the limit $\alpha \rightarrow 1$, one has $c(1) = \ln 4$. Interestingly, Eq. (III.25) shows that for n odd, $\eta_n^{(\alpha)}$ is a regular function for any value of λ , whereas for even n it diverges for $\lambda = \pm\pi/2$. This is a striking difference compared to the quench from the Néel state, for which $\eta_n^{(\alpha)}$ diverges in the limit $\lambda \rightarrow 0$ for even n (see Ref. [100]), whereas it is regular for odd n .

Also, at the leading order in z , one has that $\Phi_n^{(\alpha)} = 0$. By combining the results in (III.25) and (III.24) with the TBA equations (II.19), the leading order of the rapidity densities $\rho_{t,n}^{(\alpha)}$ are

$$\rho_{t,1}^{(\alpha)} = \frac{1}{2\pi} (1 + 4 \cos(2\lambda) z) + O(z^{\min(2,2\alpha)}), \quad (\text{III.27})$$

$$\rho_{t,2}^{(\alpha)} = \frac{1}{8\pi} + O(z^{\min(1,2\alpha)}), \quad (\text{III.28})$$

$$\rho_{t,n}^{(\alpha)} = O(z^{2\alpha}) \quad (n \geq 2). \quad (\text{III.29})$$

Notice that for any α , only $\rho_n^{(\alpha)}$ and $\rho_{t,n}^{(\alpha)}$ with $n \leq 2$ remain finite in the limit $z \rightarrow 0$, whereas all densities with $n > 2$ vanish. This is different from the Néel state, for which only the densities with $n = 1$ are finite [100]. Physically, this is expected because in the dimer state only components with at most two aligned spins can be present. Furthermore, the leading order of $\rho_{t,n}^{(\alpha)}$ in (III.27)-(III.29) does not depend on the Rényi index α . Finally, in the limit $z \rightarrow 0$, the densities become constant, similar to free-fermion models. This suggests that in the limit $z \rightarrow 0$ the form of the Rényi entropies may be similar to that of free models, as we are going to show in the following.

It is now straightforward to derive the leading behaviour of the Rényi entropies for any α in the limit $z \rightarrow 0$. First, we obtain the expansion of the driving functions g_n (III.19) as

$$g_1(\lambda) = \ln(4 \tan^2(\lambda)) + 4z + 4 \sin^2(2\lambda)z^2 + O(z^3), \quad (\text{III.30})$$

$$g_2(\lambda) = \ln(64 \sin^2(2\lambda)) + 16 \sin^2(\lambda)z + 4z^2 + O(z^3). \quad (\text{III.31})$$

The contributions of g_n for $n > 2$ are subleading for $z \rightarrow 0$ and may be neglected. Using the expansions (III.30) (III.31), the leading order of the densities in (III.27)-(III.29), and (III.25), one obtains the $z \rightarrow 0$ limit of \mathcal{E} (cf. (III.6)) as

$$\mathcal{E} = \frac{L}{4\pi} \left[\int_0^{\pi/2} d\lambda \frac{\ln(4|\tan(\lambda)|^2)}{1 + |\tan(\lambda)|^{2\alpha}} + \frac{1}{4} \int_0^{\pi/2} d\lambda \ln(64|\sin(2\lambda)|^2) \right] = \frac{L}{8} \ln(2) + \frac{L}{4\pi} \int_0^{\pi/2} d\lambda \frac{\ln(4|\tan(\lambda)|^2)}{1 + |\tan(\lambda)|^{2\alpha}}. \quad (\text{III.32})$$

The two terms in the right-hand-side of (III.32) are the contributions of the densities with $n = 1$ and $n = 2$. Similarly, the $z \rightarrow 0$ limit of the Yang-Yang entropy (II.14) is obtained as

$$S_{\text{YY}} = \frac{L}{2\pi} \int_{-\pi/2}^{\pi/2} d\lambda \left(\frac{1}{1 + |\tan(\lambda)|^{2\alpha}} \ln(1 + |\tan(\lambda)|^{2\alpha}) + \frac{1}{1 + |\cot(\lambda)|^{2\alpha}} \ln(1 + |\cot(\lambda)|^{2\alpha}) \right). \quad (\text{III.33})$$

Plugging Eq. (III.32)-(III.33) into the definition of the Rényi entropies (III.2), one obtains at the leading order in z

$$S_{\text{GGE}}^{(\alpha)} = \frac{L}{1 - \alpha} \int_{-\pi/2}^{\pi/2} \frac{d\lambda}{2\pi} \ln \left[\left(\frac{1}{1 + \tan^2(\lambda)} \right)^\alpha + \left(1 - \frac{1}{1 + \tan^2(\lambda)} \right)^\alpha \right]. \quad (\text{III.34})$$

Eq. (III.34) shows that for any α the Rényi entropies are not vanishing in the limit $z \rightarrow 0$.

The Rényi entropy obtained from (III.34) are plotted in Fig. 2 as a function of the Rényi index α . Like for finite Δ , the Rényi entropies are monotonically decreasing functions of α . For some values of α the integrals in (III.34) can be computed analytically. For instance, for the max entropy, i.e., in the limit $\alpha \rightarrow 0$, one obtains $S^{(0)}/L = \ln(2)/2$: since the max entropy is twice the logarithm of the total number of eigenstates that have nonzero overlap with the initial state [97], we have that this number is $\propto e^{L/2}$ (which is the same result for the quench from the Néel state [100]). For the min entropy we have $S^{(\infty)}/L = \ln(2) - 2G/\pi$, where G is the Catalan constant. Some other analytical results are reported in the Figure.

It is relatively easy to obtain the higher-order corrections in powers of z for any *fixed* α . Instead, it is rather cumbersome to carry out the expansion for general real α . Therefore, here we only show the explicit calculation for the case $\alpha = 2$. Specifically, we determine $S^{(2)}$ up to $\mathcal{O}(z^2)$. For convenience, instead of $\eta_n^{(\alpha)}$ we consider the filling functions $\vartheta_n \equiv 1/(1 + \eta_n)$, where we suppressed the dependence on α , because we consider $\alpha = 2$. The derivation of the higher-order expansion for the filling functions is the same as in Ref. [100] and we will omit it. The idea is that one has to plug the ansatz (III.21) into the equations for η_n (cf. (III.11)) solving the system order by order in powers of z . Similar to the Néel quench, we observe that the system (III.11) contains an infinite set of equations (one for each string type). However, to obtain the filling functions up to terms $\mathcal{O}(z^\omega)$, only the first $m(\omega) \sim \omega$ equations matter because the leading order of higher strings is given by higher orders in powers of z . The expansion of the filling functions ϑ_n around $z = 0$ reads

$$\vartheta_1(\lambda) = \frac{1}{1 + \tan(\lambda)^4(\lambda)} - \frac{16 \cos(2\lambda) \tan^4(\lambda)}{(1 + \tan^4(\lambda))} z^2 + O(z^3), \quad (\text{III.35})$$

$$\vartheta_2(\lambda) = 1 + O(z^4), \quad (\text{III.36})$$

$$\vartheta_n(\lambda) = O(z^4), \quad (n \geq 3). \quad (\text{III.37})$$

A similar procedure for the TBA equations for the particle densities (cf. (II.19)) gives

$$\rho_{t,1} = \frac{1}{2\pi} + \frac{2}{\pi} \cos(2\lambda)z + \frac{2}{\pi} \cos(4\lambda)z^2 + O(z^3), \quad (\text{III.38})$$

$$\rho_{t,2} = \frac{1}{8\pi} + \frac{2 - \sqrt{2}}{\pi} \cos^2(\lambda)z + \frac{1}{\pi} \cos(2\lambda)z^2, \quad (\text{III.39})$$

$$\rho_{t,n} = O(z^4), \quad (n \geq 3). \quad (\text{III.40})$$

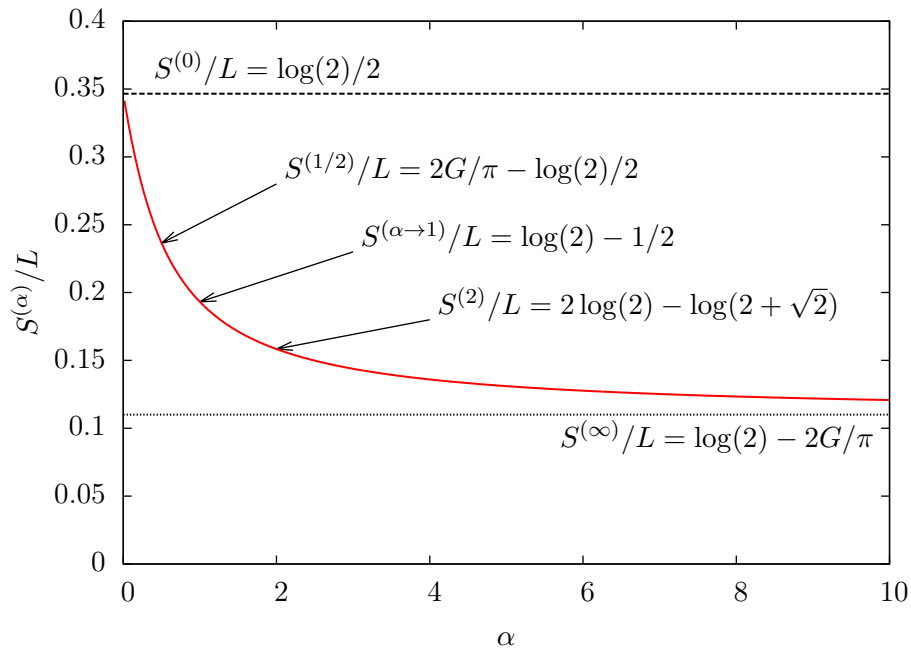


FIG. 2. Rényi entropy densities S^α/L after the quench from the dimer state in the Ising limit $\Delta \rightarrow \infty$ of the XXZ chain. On the x -axis α is the Rényi index. The results are obtained using (III.34). The dashed and the dotted lines show the max entropy $S^{(0)}$ and the min entropy $S^{(\infty)}$, respectively. Here G is the Catalan constant.

The next-to-leading order in powers of z of the Rényi entropies can be computed by plugging (III.23)(III.30)(III.31) and (III.35)-(III.40) into (III.6) and (II.14). Given that the first-order in z cancels in both \mathcal{E} and the Yang-Yang entropy and also that the $\mathcal{O}(z^2)$ contribution to S_{YY} vanishes, the first nonzero contribution is $\mathcal{O}(z^2)$ in \mathcal{E} , i.e.

$$\mathcal{E} = \frac{1}{4} \ln 2 - \frac{\sqrt{2}\pi}{32} + \frac{z^2}{2} + \mathcal{O}(z^3). \quad (\text{III.41})$$

Thus, putting the various pieces together, the second Rényi entropy $S^{(2)}$ is given as

$$S^{(2)} = 2 \ln 2 - \ln(2 + \sqrt{2}) + 2z^2 + \mathcal{O}(z^3). \quad (\text{III.42})$$

Eq. (III.42) implies that the asymptotic value of $S^{(2)}$ for $\Delta \rightarrow \infty$ is approached as $1/\Delta$.

D. A tempting but wrong conjecture

It is tempting to investigate the structure of Eq. (III.34) which has the same structure as the Rényi entropy of free-fermion models, written usually as

$$S_{\text{GGE}}^{(\alpha)} = \frac{L}{1-\alpha} \int_{-\pi/2}^{\pi/2} \frac{dk}{2\pi} \ln [\vartheta(k)^\alpha + (1 - \vartheta(k))^\alpha], \quad (\text{III.43})$$

where $\vartheta(k)$ are now the free-fermion occupation numbers identifying the macrostate. Eq. (III.43) is the same as (III.34) after defining $\vartheta(k) = 1/(1 + \tan^2(k))$. Also, the factor $1/(2\pi)$ in (III.34) is the fermionic total density of states $\rho_t = 1/(2\pi)$. A natural question is whether the free-fermion formula (III.43) holds true beyond the leading order in z . For instance, it is interesting to check whether (III.42) can be written in the free-fermion form (III.43). However, as the XXZ chain is interacting, Eq. (III.43) requires some generalisation. First, as there are different families of strings it is natural to sum over the string content of the macrostate. Moreover, in contrast with free fermions, for Bethe ansatz solvable models the total density of states ρ_t is not constant, but it depends on the string type. The most natural generalisation of the free-fermion formula (III.43) would be

$$S_{\text{GGE}}^{(\alpha)} \stackrel{?}{=} \frac{L}{1-\alpha} \sum_n \int_{-\pi/2}^{\pi/2} d\lambda \rho_{n,t} \ln [\vartheta_n^\alpha + (1 - \vartheta_n)^\alpha]. \quad (\text{III.44})$$

Eq. (III.44) is the same as the free-fermion formula (III.43) except for the overall term $\rho_{t,n}$ in the integrand, which takes into account that for interacting models the density of states is not constant. In Eq. (III.44), the filling functions are given in (III.35)-(III.37).

Unfortunately, Eq. (III.44) does not give the correct value for the steady-state Rényi entropies. A very simple counterexample is provided by the standard Gibbs ensemble at infinite temperature. For the XXZ chain the macrostate describing this ensemble can be derived using the standard TBA approach (see [103]). In particular, for the XXX chain the exact infinite temperature Rényi entropies can be worked out analytically: they become equal and their density is $S^{(\alpha)} = L \ln 2$ for any α . However, by using the analytical expression [103] for the infinite-temperature filling functions ϑ_n for the XXX chain in Eq. (III.44), one can verify that $S^{(2)}/L \neq \ln 2$.

Still, since the free-fermion formula (III.44) holds true exactly at $\Delta \rightarrow \infty$ (cf. (III.42)), it is natural to wonder at which order in $1/\Delta$ (equivalently in z) it breaks down. By using Eq. (III.38)-(III.40) and (III.35)-(III.37) in (III.44), one can check that $\rho_{t,2}$ (cf. Eq. (III.39)) gives rise to an $\mathcal{O}(z)$ term in the entropy, which is absent in (III.42). This shows that (III.44) breaks down already at the first nontrivial order beyond the Ising limit.

E. The min entropy

In this section we discuss the Rényi entropy in the limit $\alpha \rightarrow \infty$ also known as min entropy, for which analytical results are obtainable. The analysis of the min entropy after the dimer quench is similar to that for the Néel quench [100]. In the following we remove the dependence on α in the saddle point densities to simplify the notation. After defining the functions $\gamma_n = \ln(\eta_n)/\alpha$, the $\alpha \rightarrow \infty$ limit of the saddle-point equations (III.11) yields

$$\gamma_n = d_n + s \star (\gamma_{n-1}^+ + \gamma_{n+1}^+), \quad (\text{III.45})$$

where $\gamma_n^+ = (\gamma_n + |\gamma_n|)/2$. Some insights on the structure of the solutions of (III.45) can be obtained by looking at the limit $\Delta \rightarrow \infty$. Precisely, from Eq. (III.25) one has that $\eta_n \rightarrow 0$ for even n in the limit $\alpha \rightarrow \infty$. On the other hand, one has that η_n diverges for odd n for $\lambda \in [-\pi/4, \pi/4]$, which implies $\ln \eta_n = \alpha d_n$ for n odd in that interval. Thus we have that at large Δ , $\gamma_{2n}(\lambda) < 0$ and $\gamma_{2n+1}(\lambda) = d_{2n+1}(\lambda)$. As a consequence, the filling functions ϑ_n become

$$\vartheta_{2n}(\lambda) = \lim_{\alpha \rightarrow \infty} \frac{1}{1 + e^{\alpha \gamma_{2n}(\lambda)}} = 1, \quad (\text{III.46})$$

$$\vartheta_{2n+1}(\lambda) = \lim_{\alpha \rightarrow \infty} \frac{1}{1 + e^{\alpha d_{2n+1}(\lambda)}} = \Theta_{\text{H}}(|\lambda| - \pi/4), \quad (\text{III.47})$$

where $\Theta_{\text{H}}(x)$ is the Heaviside step function. The associated total densities are obtained using the BGT equations as

$$\rho_{t,1}(\lambda) = s(\lambda), \quad (\text{III.48})$$

$$\rho_{t,2}(\lambda) = [s \star (s \cdot \Theta_{\text{H}}(|x| - \pi/4))](\lambda) \quad (\text{III.49})$$

$$= \frac{1}{4\pi^2} \sum_{k \in \mathbb{Z}} \frac{e^{-2ik\lambda}}{\cosh(k\eta)} \left(\sum_{\ell \neq k} \frac{\sin((k-\ell)\pi) - \sin((k-\ell)\pi/2)}{(k-\ell) \cosh(\ell\eta)} + \frac{\pi}{2 \cosh(k\eta)} \right),$$

$$\rho_{t,n}(\lambda) = 0, \quad (n > 2). \quad (\text{III.50})$$

These results imply that the min entropy is completely determined by the first two densities with $n = 1$ and $n = 2$, in contrast with the quench from the Néel state [100], where only the first density enters in the expression for $S^{(\infty)}$.

To derive the general expression for the min entropy, a crucial preliminary observation is that the macrostate describing $S^{(\infty)}$ has zero Yang-Yang entropy. This is a general result that holds for quenches from arbitrary states. Indeed, first we notice that the ansatz $\eta_n = e^{\alpha \gamma_n}$ implies that, in the limit $\alpha \rightarrow \infty$, ϑ_n can be only zero or one. Then, assuming that $\rho_{t,n}$ is finite, the Yang-Yang entropy

$$S_{YY} = -L \sum_n \int d\lambda \rho_{t,n} [\vartheta_n \ln \vartheta_n + (1 - \vartheta_n) \ln(1 - \vartheta_n)], \quad (\text{III.51})$$

must vanish in the limit $\alpha \rightarrow \infty$. Consequently the $S_{\text{GGE}}^{(\infty)}$ is determined only by the driving functions as

$$S_{\text{GGE}}^{(\infty)} = L \sum_n \int_{-\pi/2}^{\pi/2} d\lambda g_n \rho_n + L f_{\text{GGE}}. \quad (\text{III.52})$$

Interestingly, in the large Δ limit Eq. (III.52) simplifies. Specifically, only the first two strings with $n = 1, 2$ contribute in (III.52), as it is clear from (III.50).

Upon lowering Δ , we observe a sharp transition in the behaviour of $S^{(\infty)}$. Indeed, there is a ‘‘critical’’ value Δ^* , such that for $\Delta < \Delta^*$, higher-order strings become important. The condition that determines Δ^* is that γ_2 becomes positive, i.e., that for some λ

$$d_2 + 2s \star d_1 \geq 0. \quad (\text{III.53})$$

The value of Δ^* can be found by numerically by imposing equality in (III.53) and the final result is $\Delta^* \approx 1.7669$. This is the same value of Δ^* found for the quench from the Néel state [100], although the condition for higher strings to contribute for the Néel state (i.e. $d_1 + 2s \star d_2 \geq 0$) may appear different. This, however, is equivalent to (III.53) after noticing that $d_{2n}^{\text{Dimer}} = d_{2n+1}^{\text{Néel}}$.

Finally, in contrast with the large Δ limit, for $\Delta < \Delta^*$, an analytical solution of (III.45) is not possible. However, the system (III.45) can be effectively solved numerically. The result for $S^{(\infty)}$ is reported in Figure 1 (bottom line).

IV. RÉNYI ENTROPIES OF GENERIC THERMODYNAMIC MACROSTATES

In this section we show how to generalise the approach of Ref. [97] for the calculation of Rényi entropies in the case when the overlaps of a given initial state are not known. In this case, we just know the rapidity densities of the macrostate, e.g. from the generalised Gibbs ensemble construction [50, 101]. The key idea is embarrassing simple: using the TBA equations (cf. (III.9) for $\alpha = 1$)

$$\ln \eta_n = g_n + \sum_{m=1}^{\infty} A_{nm} \star \ln[1 + 1/\eta_m], \quad (\text{IV.1})$$

we can extract the numerical values of the driving functions $g_n(\lambda)$ from the saddle point solutions $\eta_n(\lambda)$. Once the driving functions are numerically known, it is straightforward to use them in the formalism of Ref. [97] to obtain the steady-state Rényi entropies, as explained in the previous sections. Notice that this procedure does not only apply to stationary states after a quench, but can be used for *generic* Bethe states with arbitrary root densities, independently of where they come from. Furthermore, for quench problems, this procedure can be used to reconstruct the extensive part of the overlaps and hence to help in conjecturing the entire overlap function at finite size.

To illustrate the validity of the approach, in the following subsections we provide exact results for the Rényi entropies after the quench from the tilted Néel state in the XXZ chain. For this family of quenches, the thermodynamic macrostates describing the post-quench steady states have been calculated in Ref. [101] from the GGE. Only very recently (and after most of this paper was completed) the overlaps of these states with the Bethe ones have been conjectured in Ref. [102]. Consequently, the results presented in the following, not only are a physical relevant application of these ideas but also provide a further confirmation about the validity of the conjecture itself. Finally, we mention that if these ideas would have been developed earlier, they could have speed up the formulation of the conjecture in [102].

A. Quench from the tilted Néel: Extracting the driving

Here we numerically extract the driving functions $g_n(\lambda)$ for the quench from the tilted Néel state. The key ingredients are the rapidity densities describing the post-quench steady state that have been determined in Ref. [101]. These are used in the system (IV.1) to extract g_n . To make the paper self contained, we report the results for the saddle point densities. The starting point is $\eta_1(\lambda)$, which is given as

$$\eta_1(\lambda) = -1 + \frac{T_1(\lambda + i\frac{\eta}{2}) T_1(\lambda - i\frac{\eta}{2})}{\phi(\lambda + i\frac{\eta}{2}) \bar{\phi}(\lambda - i\frac{\eta}{2})}, \quad (\text{IV.2})$$

where the auxiliary functions $\phi, \bar{\phi}$ and T_1 are defined as

$$T_1(\lambda) = -\frac{1}{8} \cot(\lambda) \{8 \cosh(\eta) \sin^2(\theta) \sin^2(\lambda) - 4 \cosh(2\eta) + [\cos(2\theta) + 3][2 \cos(2\lambda) - 1] + 2 \sin^2(\theta) \cos(4\lambda)\}, \quad (\text{IV.3})$$

$$\phi(\lambda) = \frac{1}{8} \sin(2\lambda + i\eta) [2 \sin^2(\theta) \cos(2\lambda - i\eta) + \cos(2\theta) + 3], \quad (\text{IV.4})$$

$$\bar{\phi}(\lambda) = \frac{1}{8} \sin(2\lambda - i\eta) [2 \sin^2(\theta) \cos(2\lambda + i\eta) + \cos(2\theta) + 3]. \quad (\text{IV.5})$$

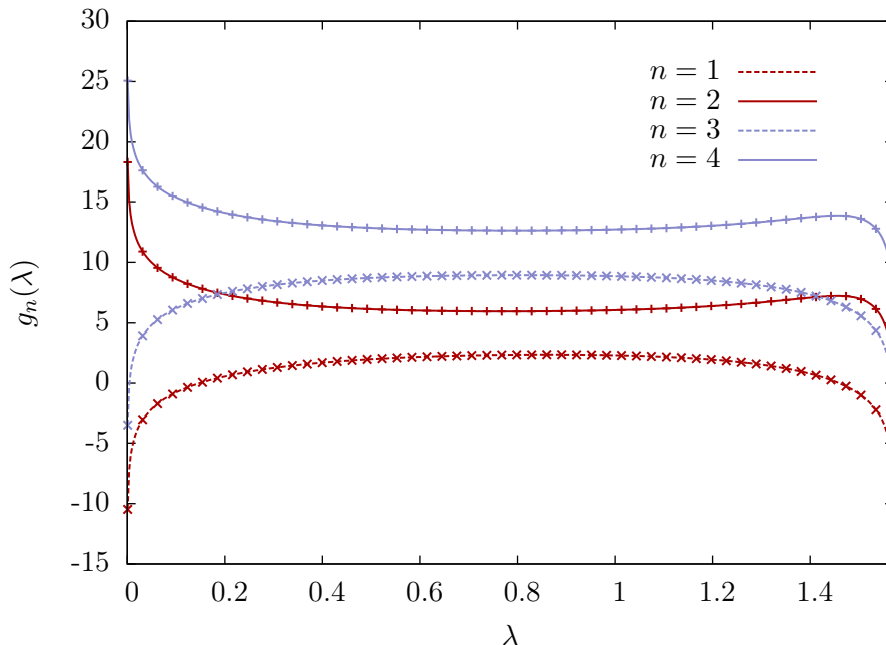


FIG. 3. GGE driving functions g_n for the quench from the tilted Néel state in the XXZ chain with $\Delta = 2$. On the x -axis λ is the rapidity variable. The Néel tilting angle is $\theta = \pi/3$. Different lines correspond to different strings lengths n . Lines are numerical results using the TBA approach, whereas points denote the analytical conjecture in Ref. [102].

Here θ denotes the tilting angle. For $n > 1$, $\eta_n(\lambda)$ is determined recursively from the Y-system

$$\eta_{n+1}(\lambda) = \frac{\eta_n(\lambda + i\eta/2)\eta_n(\lambda - i\eta/2)}{1 + \eta_{n-1}(\lambda)} - 1, \quad (\text{IV.6})$$

with the convention $\eta_0 \equiv 0$. From the densities η_n , the particle densities ρ_n are obtained, as usual, by solving the thermodynamic version of the TBA equations (II.15).

The driving function g_n can be easily extracted numerically by plugging the above root densities in Eq. (IV.1). The results for quenches for the XXZ chain with $\Delta = 2$ and the quench from the tilted Néel state with tilting angle $\theta = \pi/3$ are reported in Figure 3. These results may be compared with the recently conjectured form of the overlaps [102]. So far, this conjecture has been tested numerically for Bethe states containing few particles, and it has been shown to give the correct thermodynamic macrostate after the quench. The thermodynamic limit of the overlaps in [102] can be written as

$$\ln\langle\Psi_0|\rho_n\rangle = L \sum_{n=1}^{\infty} \int_{-\pi/2}^{\pi/2} d\lambda \rho_n(\lambda) g_n(\lambda), \quad (\text{IV.7})$$

where ρ_n are the particle densities describing the thermodynamic macrostate and the explicit forms of g_n read [102]

$$g_1(\lambda) = \frac{\tan(\lambda + i\eta/2) \tan(\lambda - i\eta/2)}{4 \sin^2(2\lambda)} \cdot \frac{\cos^2(\lambda + i\xi) \cos^2(\lambda - i\xi)}{\cosh^4(\xi)}, \quad (\text{IV.8})$$

$$g_n(\lambda) = \sum_{j=1}^n g_1(\lambda + i\eta/2(n+1-2j)), \quad (\text{IV.9})$$

where ξ is related to the tilting angle θ as $\xi \equiv -\ln(\tan(\theta/2))$.

We now compare the driving functions g_n as extracted from the TBA equations (IV.1) with the conjectured result in Eq. (IV.8) and (IV.9). The comparison is presented in Figure 3 for the XXZ chain with $\Delta = 2$ and the quench from the tilted Néel state with tilting angle $\theta = \pi/3$ (we tested them also for other tilting angles, finding equivalent results that we do not report here). The continuous lines are the numerical results for g_n for $n \leq 4$ (higher strings are not reported). The different symbols (crosses) are the numerical results using the conjecture (IV.8)-(IV.9). As it is clear from the Figure, the agreement between the two results is perfect for all values of λ .

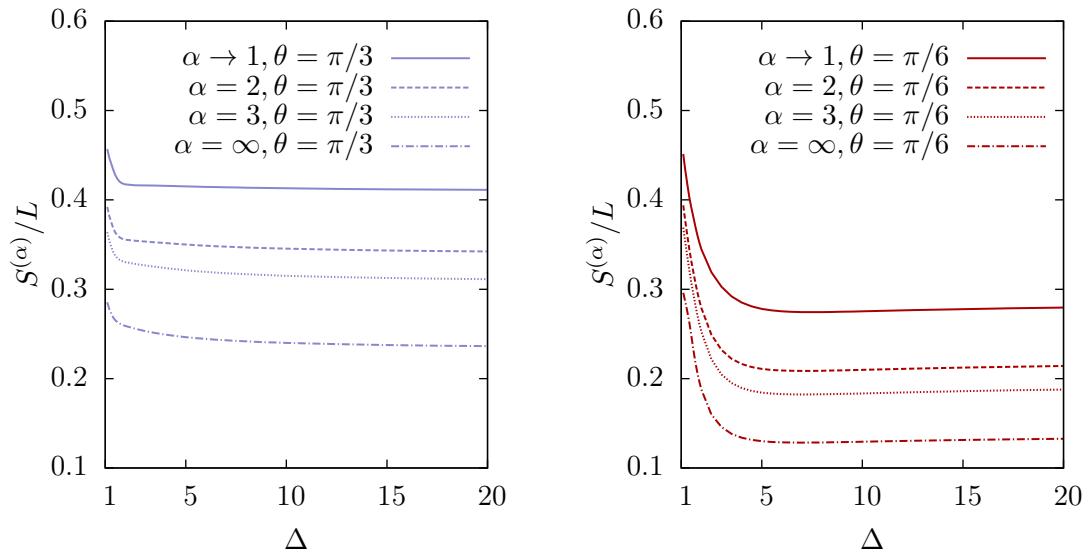


FIG. 4. Steady-state Rényi entropies $S^{(\alpha)}/L$ after the quench from the tilted Néel state in the XXZ spin chain. The entropies are plotted as a function of the anisotropy Δ . We show results for tilting angles $\theta = \pi/6$ and $\theta = \pi/3$ (right and left panel, respectively). In each panel the different curves correspond to different values of $\alpha \in [1, \infty)$.

B. Rényi entropies after quenching from the tilted Néel state

Now we are in the position to obtain results for the steady-state Rényi entropies after the quench from the tilted Néel state in the XXZ chain. The theoretical predictions for the entropies are obtained by combining the results of section IV A to extract the driving functions g_n with the procedure of Ref. [97] (see section III). Our results are reported in Figure 4 plotting $S^{(\alpha)}/L$ versus the chain anisotropy Δ . The data shown in the Figure are for the tilted Néel with tilting angle $\theta = \pi/3$ and $\theta = \pi/6$ (right and left panel, respectively). As expected, one has that $S^{(\alpha)} < S^{(\alpha')}$ if $\alpha > \alpha'$. For all values of α and $\theta \neq 0$ the entropy densities are finite in the limit $\Delta \rightarrow \infty$, in contrast with the quench from the Néel state [100], where all the entropies vanish for $\Delta \rightarrow \infty$. Finally, an intriguing feature is that for $\theta = \pi/6$ the behaviour of the entropies is not monotonic as a function of Δ , but $S^{(\alpha)}$ exhibits a minimum around $\Delta \approx 5$, although the minimum is not very pronounced. This remains true for a window of tilting angle θ close to $\pi/6$.

C. The min entropy

We now focus on the steady-state value of the min entropy. Similar to the Néel and dimer states, in the limit $\alpha \rightarrow \infty$ one can use the ansatz $(\ln \eta_n)/\alpha = \gamma_n$. The equations for γ_n are the same as for the dimer (cf. (III.45)), i.e.,

$$\gamma_n = d_n + s \star (\gamma_{n-1}^+ + \gamma_{n+1}^+), \quad (\text{IV.10})$$

where now the driving d_n is obtained from the driving functions g_n for the quench from the tilted Néel as

$$d_n = g_n - s \star (g_{n+1} + g_{n-1}). \quad (\text{IV.11})$$

For the Néel quench, i.e., for $\theta = 0$, there is a “critical” value Δ^* such that for $\Delta > \Delta^*$ the thermodynamic macrostate that describes the min entropy is the ground state of the XXZ chain [100]. For $\Delta < \Delta^*$ this is not the case, and the macrostate is an excited state with zero Yang-Yang entropy. The “critical” Δ^* at which the behaviour of the thermodynamic macrostate changes is determined for the Néel state (and for the dimer state as well) by the condition that γ_2 becomes positive. It is natural to investigate how this scenario is modified upon tilting the initial state. Here we show that the macrostate describing the min entropy is the ground state of the XXZ chain provided that the tilting angle θ is not too large.

To clarify this issue, we numerically observed that for large Δ

$$\begin{aligned} \gamma_1(\lambda) &< 0, \\ \gamma_3(\lambda) &< 0. \end{aligned} \quad (\text{IV.12})$$

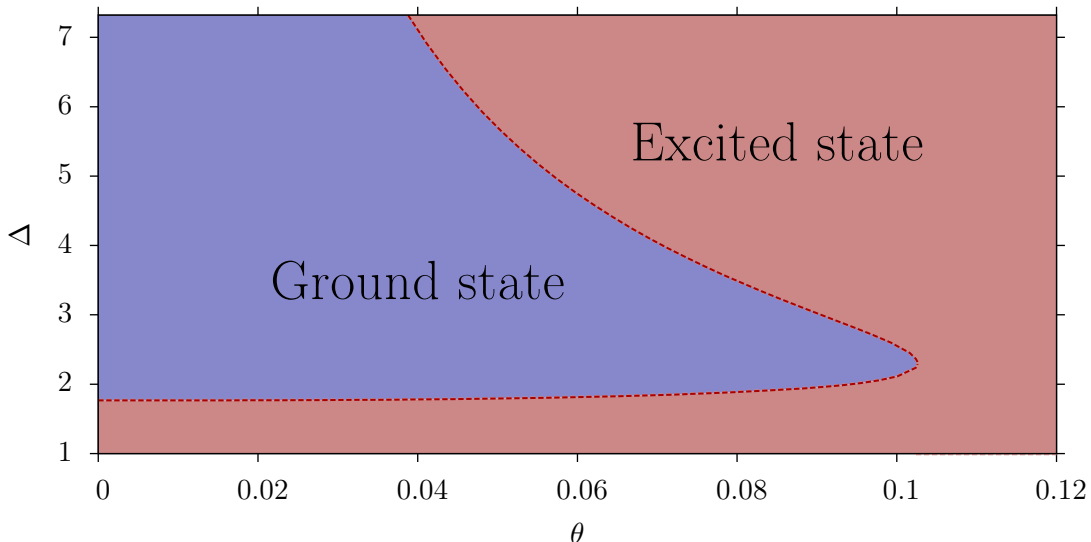


FIG. 5. TBA macrostate for the steady-state value of the min entropy $S^{(\infty)}$ after the quench from the tilted Néel state in the XXZ chain. The Figure show the macrostate as a function of the chain anisotropy Δ and the tilting angle θ . The blue area denotes the parameter region (θ, Δ) where the macrostate is the ground state of the XXZ chain at that Δ . Outside this region, the macrostate is an excited state of the chain. The dashed line divides the two regions.

The conditions in Eq. (IV.12) have important consequences for the particle densities ρ_n . In particular, it implies that the macrostate describing the min entropy is the ground state of the XXZ chain. To show that, let us consider the TBA equations for $\rho_{t,n}$

$$\rho_{n,t} = s \star [(1 - \vartheta_{n-1})\rho_{n-1,t} + (1 - \vartheta_{n+1})\rho_{n+1,t}]. \quad (\text{IV.13})$$

First, since $\vartheta_0 = 0$ and $\rho_0 = \delta(\lambda)$, one has that $\rho_1 = s$, which is the density of the ground state of the XXZ chain. Clearly, the conditions in (IV.12) together with the system (IV.13) imply that $\rho_{2,t} = 0$. Another important consequence is that the first two equations in (IV.13) are decoupled from the rest, which form a linear homogeneous system of integral equations. Moreover, for $n \rightarrow \infty$ one expects that $\rho_{t,n} \rightarrow 0$. Thus, it is natural to conjecture that $\rho_{t,n} = 0$ for any $n > 2$. Finally, we observe that a similar decoupling occurs for the quench from the Néel state [100], although via a different mechanism. Precisely, for the the Néel state one has that $\gamma_{2n+1} < 0$ for all n .

We now use the conditions (IV.12) to characterise the behaviour of the min entropy. Our results are summarised in the “phase diagram” in Fig. 5. The blue region in the figure corresponds to the region in the parameter space (θ, Δ) where the thermodynamic macrostate describing the min entropy is the ground state of the XXZ chain (at that value of Δ). For $\theta = 0$ we recover the result of Ref. [100], i.e., that the ground state describes the min entropy for $\Delta > \Delta^* \approx 1.766$. The ground state remains the correct macrostate for the min entropy in a region of not too large θ . Conversely, for $\theta \gtrsim 0.1$ the macrostate is an excited state of the XXZ at any Δ . However, at smaller θ there is always an extended region where the min entropy is described by the ground state of the XXZ chain. The extension of this region shrinks upon increasing Δ , and it is likely to vanish in the limit $\Delta \rightarrow \infty$. The dashed line in Fig. 5 marks the “transition” between the two regimes. The line is obtained by numerically finding the values of (θ, Δ) for which either γ_1 or γ_3 vanish, violating the conditions in Eq. (IV.12).

V. NUMERICAL BENCHMARKS USING TDMRG

In this section we exploit the equivalence between the reduced density matrices in the thermodynamic ensemble (the GGE in our case) and in the long time limit after a quench to provide numerical confirmations of the results of the previous section by means of entanglement entropy dynamics. We employ tDRMG [128–131] simulations in the framework of the Matrix Product States (MPS) [132]. The tilted Néel state is conveniently constructed by first constructing the Néel state, which admits a simple MPS representation with bond dimension $\chi = 1$. The tilted Néel is then obtained by applying a global rotation site by site, by using the Matrix Product Operator representation of the spin rotation operator $\exp(i\theta \sum_i \sigma_i^y)$. The time evolution is implemented by using a standard second order Trotter-Suzuki approximation of the time evolution operator $\exp(-iHt)$, with a time step $\delta t = 0.02$. At each application of

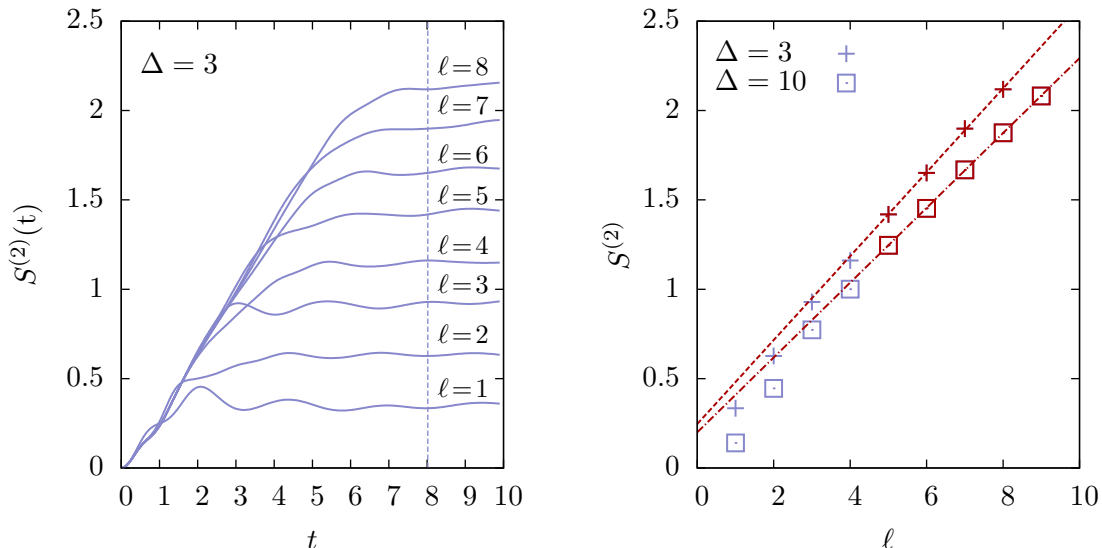


FIG. 6. Testing TBA results for the steady-state Rényi entropies against tDMRG simulations in the XXZ chain. The system is quenched from the tilted Néel state with different values of the chain anisotropy Δ and tilting angle θ . Left panel: tDMRG data for the second Rényi entanglement entropy $S^{(2)}$ at $\Delta = 3$ plotted as a function of time. Different lines are for different sizes ℓ of the subsystem. Right panel: Saturation values of the entropy density $S^{(2)}$ at long time (i.e. data at $t = 8$, corresponding to the vertical line in the left panel). The entropy density (symbols in the figure) is plotted versus ℓ . The lines are linear fits to $a\ell + b$. Only the red symbols are included in the fit. The fit gives $a \approx 0.23$ and $a \approx 0.21$ for $\Delta = 10$ and $\Delta = 3$, respectively. These values are compatible with the TBA results $S^{(2)}/\ell \approx 0.2321$ for $\Delta = 3$ and $S^{(2)}/\ell \approx 0.2098$ for $\Delta = 10$.

the time evolution the bond dimension χ grows. To keep χ reasonably small, at each time step we perform a truncated Singular Value Decomposition (SVD) of each tensor forming the MPS. Specifically, in the SVD we keep the largest χ_{\max} singular values, with $\chi_{\max} \approx 100$. For the quenches that we consider we verified that this is sufficient to obtain accurate results up to times $t \approx 10$.

Our numerical results are shown in Figure 6. The left panel shows the second Rényi entropy $S^{(2)}$ plotted as a function of time. The data are tDMRG results for the quench from the tilted Néel state in the XXZ chain for tilting angle $\theta = \pi/6$ and $\Delta = 3$. The different lines correspond to different subsystem sizes ℓ . The right panel shows the saturation value of $S^{(2)}$ as a function of ℓ . Precisely, for $\Delta = 3$ the data correspond to $t \approx 8$ (see vertical line in the left panel). The different symbols correspond to different values of Δ . The expected volume-law behaviour $S^{(2)} \propto \ell$ is clearly visible. The lines are linear fits to $a\ell + b$, with a, b fitting parameters. Only the largest sizes ℓ are included in the fit (red symbols in the Figure). The fit gives $a \approx 0.23$ and $a \approx 0.21$ for $\Delta = 3$ and $\Delta = 10$, respectively. These results are in excellent agreement with the TBA predictions $a \approx 0.2321$ and $a = 0.2098$ (see Figure 4 for the predictions).

VI. CONCLUSIONS

In this manuscript we studied the Rényi entropies in the stationary state after a quantum quench. As shown in Refs. [97, 100], in the quench action approach the Rényi entropies are generalised free energy of a macrostate that may be derived from the knowledge of the overlaps of the initial state with Bethe eigenstates. The thermodynamic limit of the overlaps provides the driving term in the TBA formalism. Here we considered the problem of determining the Rényi entropies in a generic thermodynamic macrostate of integrable models, even in those cases when the overlaps are not known. We showed that the needed driving term can be reconstructed starting from the macrostate's particle densities. Then we provided a major simplification of the expression for the generalised free energy that may be rewritten only as a function of the occupation numbers of one-strings, cf. Eq. (III.18) which is a much simpler and manageable formula than the known sum over all string content.

We then studied accurately the stationary Rényi entropies after the quench from the dimer and the tilted Néel states in the XXZ Heisenberg spin chain. For the former initial state we employed the overlap TBA approach, while for the latter we reconstructed the driving terms from the macrostate. The overall results for the dimer states are summarised in Fig. 1 which shows the Δ and α dependence of the Rényi entropies. We also analysed in details two

limits that are analytically tractable, namely $\Delta \rightarrow \infty$ and $\alpha \rightarrow \infty$. In the Ising limit $\Delta \rightarrow \infty$, the result for the Rényi entropies resembles that of free-fermion models, as it should. Deviations from the free-fermion result appear already at the first non trivial order in $1/\Delta$. For the min entropy, i.e. $\alpha \rightarrow \infty$, we found that the representative state has vanishing Yang-Yang entropy for arbitrary Δ . We also found a sharp transition of this state at a critical value of Δ denoted as Δ^* . For $\Delta > \Delta^*$, the representative state contains one- and two-strings only (as a difference with the quench from Néel state where only one-strings matter) while for $\Delta < \Delta^*$ the other bound states start being present. When the initial configuration is the tilted Néel state, the results for the Rényi entropies as function of Δ, α , and the tilting angle θ are reported in Fig. 4. As a main difference with the other cases, the entropies as function of Δ are not always monotonic, but they may show a minimum for some values of θ . Also in this case we analytically studied the min entropy. We again found that the representative eigenstate has zero Yang-Yang entropy for arbitrary Δ and θ and that there is a sharp transition line. The resulting "phase diagram" is reported in Fig. 5: there is a region for small θ where the representative eigenstate is the ground state (and hence only one-strings are present), while in the rest of the phase diagram, other bound states matter. The results presented here (and the ones for the Néel state [100]) show that rather generically the representative state of the min entropy has zero Yang-Yang entropy. It would be interesting to find out the minimal conditions on the initial state for this property to be generically valid.

Finally, we exploited the equivalence between thermodynamic and entanglement entropies to check by means of numerical simulations the correctness of our results. We found that the numerical data for the Rényi entanglement entropies at large time are perfectly compatible with TBA results for the thermodynamic entropies.

A major problem that remains still open is to characterise the time evolution of Rényi entanglement entropies for generic interacting integrable model, both for homogeneous quenches and quenches from piecewise homogeneous initial states (see [133] for some results). Technically, it is not possible to generalise the semiclassical approach developed for the von Neumann entropy [8, 9] because the Rényi entropies have been written in terms of root distributions which are not the ones of the macrostate describing local properties: only the latter determines the asymptotic spreading of entanglement [8, 9] and correlations [134]. Apart from the *per se* theoretical interest, this issue is also fundamental for a comparison with cold atom experiments in which only Rényi entropies can be measured [11, 94–96].

ACKNOWLEDGMENTS

M.M. thanks Balázs Pozsgay for inspiring discussions. V.A. acknowledges support from the European Union's Horizon 2020 under the Marie Skłodowska-Curie grant agreement No 702612 OEMBS. Part of this work has been carried out during the workshop "Quantum paths" at the Erwin Schrödinger International Institute for Mathematics and Physics (ESI) in Vienna, and during the workshop "Entanglement in Quantum Systems" at the Galileo Galilei Institute (GGI) in Florence.

-
- [1] N. Schuch, M. M. Wolf, F. Verstraete, and J. I. Cirac, Entropy scaling and simulability by Matrix Product States, *Phys. Rev. Lett.* **100**, 030504 (2008);
N. Schuch, M. M. Wolf, K.G. H. Vollbrecht, and J. I. Cirac, On entropy growth and the hardness of simulating time evolution, *New J. Phys.* **10**, 033032 (2008).
 - [2] A. Perales and G. Vidal, Entanglement growth and simulation efficiency in one-dimensional quantum lattice systems, *Phys. Rev. A* **78**, 042337 (2008).
 - [3] P. Hauke, F. M. Cucchietti, L. Tagliacozzo, I. Deutsch, and M. Lewenstein, Can one trust quantum simulators?, *Rep. Prog. Phys.* **75** 082401 (2012).
 - [4] J. Dubail, Entanglement scaling of operators: a conformal field theory approach, with a glimpse of simulability of long-time dynamics in 1+1d, *J. Phys. A* **50**, 234001 (2017).
 - [5] J. M. Deutsch, H. Li, and A. Sharma, Microscopic origin of thermodynamic entropy in isolated systems, *Phys. Rev. E* **87**, 042135 (2013).
 - [6] M. Collura, M. Kormos, and P. Calabrese, Stationary entropies following an interaction quench in 1D Bose gas, *J. Stat. Mech.* P01009 (2014).
 - [7] W. Beugeling, A. Andreanov, and M. Haque, Global characteristics of all eigenstates of local many-body Hamiltonians: participation ratio and entanglement entropy, *J. Stat. Mech.* (2015) P02002.
 - [8] V. Alba and P. Calabrese, Entanglement and thermodynamics after a quantum quench in integrable systems, *PNAS* **114**, 7947 (2017).
 - [9] V. Alba and P. Calabrese, Entanglement dynamics after quantum quenches in generic integrable systems, *SciPost Phys.* **4**, 017 (2018).
 - [10] A. Nahum, J. Ruhman, S. Vijay, and J. Haah, Quantum Entanglement Growth Under Random Unitary Dynamics, *Phy. Rev. X* **7**, 031016 (2017);

- A. Nahum, S. Vijay, and J. Haah, Operator Spreading in Random Unitary Circuits *Phys. Rev. X* **8**, 021014 (2018);
 A. Nahum, J. Ruhman, and D. A. Huse, Dynamics of entanglement and transport in 1D systems with quenched randomness, [arXiv:1705.10364](https://arxiv.org/abs/1705.10364).
- [11] A. M. Kaufman, M. E. Tai, A. Lukin, M. Rispoli, R. Schittko, P. M. Preiss, and M. Greiner, Quantum thermalization through entanglement in an isolated many-body system, *Science* **353**, 794 (2016).
- [12] Y. O. Nakagawa, M. Watanabe, H. Fujita, and S. Sugiura, Universality in volume law entanglement of pure quantum states, *Nat. Comm.* **9**, 1635 (2018).
- [13] A. Polkovnikov, Microscopic diagonal entropy and its connection to basic thermodynamic relations, *Ann. Phys.* **326**, 486 (2011).
- [14] L. F. Santos, A. Polkovnikov, and M. Rigol, Entropy of isolated quantum systems after a quench, *Phys. Rev. Lett.* **107**, 040601 (2011).
- [15] L. F. Santos, A. Polkovnikov, and M. Rigol, Weak and strong typicality in quantum systems, *Phys. Rev. E* **86**, 010102 (2012).
- [16] V. Gurarie, Global large time dynamics and the generalized Gibbs ensemble, *J. Stat. Mech.* (2013) P02014.
- [17] M. Fagotti, Finite-size corrections vs. relaxation after a sudden quench, *Phys. Rev. B* **87**, 165106 (2013).
- [18] M. Kormos, L. Bucciardini, and P. Calabrese, Stationary entropies after a quench from excited states in the Ising chain, *EPL* **107**, 40002 (2014);
 L. Bucciardini, M. Kormos, and P. Calabrese, Quantum quenches from excited states in the Ising chain, *J. Phys. A* **47**, 175002 (2014).
- [19] M. Rigol, Quantum Quenches in the Thermodynamic Limit, *Phys. Rev. Lett.* **112**, 170601 (2014).
- [20] M. Rigol, Fundamental Asymmetry in Quenches Between Integrable and Nonintegrable Systems, *Phys. Rev. Lett.* **116**, 100601 (2016).
- [21] L. Piroli, E. Vernier, P. Calabrese, and M. Rigol, Correlations and diagonal entropies after quantum quenches in XXZ chains, *Phys. Rev. B* **95**, 054308 (2017).
- [22] P. Calabrese and J. Cardy, Time Dependence of Correlation Functions Following a Quantum Quench, *Phys. Rev. Lett.* **96** 136801 (2006).
- [23] C. Gogolin and J. Eisert, Equilibration, thermalisation, and the emergence of statistical mechanics in closed quantum systems, *Rep. Prog. Phys.* **79**, 056001 (2016).
- [24] P. Calabrese, F. H. L. Essler, and G. Mussardo, Introduction to “Quantum Integrability in Out of Equilibrium Systems”, *J. Stat. Mech.* (2016) P064001.
- [25] F. H. L. Essler and M. Fagotti, Quench dynamics and relaxation in isolated integrable quantum spin chains, *J. Stat. Mech.* (2016) 064002.
- [26] R. V. Jensen and R. Shankar, Statistical behaviour in Deterministic Quantum Systems with Few Degrees of Freedom, *Phys. Rev. Lett.* **54**, 1879 (1985).
- [27] J. M. Deutsch, Quantum statistical mechanics in a closed system, *Phys. Rev. A* **43**, 2046 (1991).
- [28] M. Srednicki, Chaos and quantum thermalization, *Phys. Rev. E* **50**, 888 (1994).
- [29] M. Rigol, V. Dunjko, and M. Olshanii, Thermalization and its mechanism for generic isolated quantum systems, *Nature* **452**, 854 (2008).
- [30] M. Rigol and M. Srednicki, Alternatives to Eigenstate Thermalization, *Phys. Rev. Lett.* **108**, 110601 (2012).
- [31] L. D’Alessio, Y. Kafri, A. Polkovnikov, and M. Rigol, From Quantum Chaos and Eigenstate Thermalization to Statistical Mechanics and Thermodynamics, *Adv. Phys.* **65**, 239 (2016).
- [32] M. Rigol, V. Dunjko, V. Yurovsky, and M. Olshanii, Relaxation in a Completely Integrable Many-Body Quantum System: An *Ab Initio* Study of the Dynamics of the Highly Excited States of 1D Lattice Hard-Core Bosons. *Phys. Rev. Lett.* **98**, 050405 (2007).
- [33] M. A. Cazalilla, Effect of Suddenly Turning on Interactions in the Luttinger Model, *Phys. Rev. Lett.* **97**, 156403 (2006).
- [34] P. Calabrese and J. Cardy, Quantum quenches in extended systems, *J. Stat. Mech.* (2007) P06008.
- [35] T. Barthel and U. Schollwöck, Dephasing and the Steady State in Quantum Many-Particle Systems. *Phys. Rev. Lett.* **100**, 100601 (2008).
- [36] M. Cramer, C. M. Dawson, J. Eisert, and T. J. Osborne, Exact Relaxation in a Class of Nonequilibrium Quantum Lattice Systems, *Phys. Rev. Lett.* **100**, 030602 (2008).
- [37] M. Cramer and J. Eisert, A quantum central limit theorem for non-equilibrium systems: exact local relaxation of correlated states, *New J. Phys.* **12**, 055020 (2010).
- [38] M. A. Cazalilla, A. Iucci, and M.-C. Chung, Thermalization and quantum correlations in exactly solvable models, *Phys. Rev. E* **85**, 011133 (2012).
- [39] P. Calabrese, F. H. L. Essler, and M. Fagotti, Quantum Quench in the Transverse-Field Ising Chain, *Phys. Rev. Lett.* **106**, 227203 (2011);
 P. Calabrese, F. H. L. Essler, and M. Fagotti, Quantum quench in the transverse field Ising chain: I. Time evolution of order parameter correlators, *J. Stat. Mech.* (2012) P07016.
- [40] P. Calabrese, F. H. L. Essler, and M. Fagotti, Quantum quenches in the transverse field Ising chain: II. Stationary state properties, *J. Stat. Mech.* (2012) P07022.
- [41] J. Mossel and J.-S. Caux, Generalized TBA and generalized Gibbs, *J. Phys. A* **45**, 255001 (2012).
- [42] D. Fioretto and G. Mussardo, Quantum quenches in integrable field theories, *New J. Phys.* **12**, 055015 (2010);
 S. Sotiriadis, D. Fioretto, and G. Mussardo, Zamolodchikov-Faddeev algebra and quantum quenches in integrable field theories, *J. Stat. Mech.* (2012) P02017.

- [43] M. Collura, S. Sotiriadis, and P. Calabrese, Equilibration of a Tonks-Girardeau Gas Following a Trap Release, *Phys. Rev. Lett.* **110**, 245301 (2013);
M. Collura, S. Sotiriadis, and P. Calabrese, Quench dynamics of a Tonks-Girardeau gas released from a harmonic trap, *J. Stat. Mech.* (2013) P09025.
- [44] M. Fagotti and F. H. L. Essler, Stationary behaviour of observables after a quantum quench in the spin-1/2 Heisenberg XXZ chain, *J. Stat. Mech.* (2013) P07012.
- [45] B. Pozsgay, The generalized Gibbs ensemble for Heisenberg spin chains, *J. Stat. Mech.* P07003 (2013).
- [46] M. Fagotti and F. H. L. Essler, Reduced Density Matrix after a Quantum Quench, *Phys. Rev. B* **87**, 245107 (2013).
- [47] M. Kormos, M. Collura, and P. Calabrese, Analytic results for a quantum quench from free to hard-core one-dimensional bosons, *Phys. Rev. A* **89**, 013609 (2014).
- [48] S. Sotiriadis and P. Calabrese, Validity of the GGE for quantum quenches from interacting to noninteracting models, *J. Stat. Mech.* (2014) P07024.
- [49] M. Fagotti, M. Collura, F. H. L. Essler, and P. Calabrese, Relaxation after quantum quenches in the spin-1/2 Heisenberg XXZ chain, *Phys. Rev. B* **89**, 125101 (2014).
- [50] E. Ilievski, J. De Nardis, B. Wouters, J.-S. Caux, F. H. L. Essler, and T. Prosen, Complete Generalized Gibbs Ensembles in an Interacting Theory, *Phys. Rev. Lett.* **115**, 157201 (2015);
E. Ilievski, E. Quinn, J. D. Nardis, and M. Brockmann, String-charge duality in integrable lattice models, *J. Stat. Mech.* (2016) 063101.
- [51] V. Alba, Simulating the Generalized Gibbs Ensemble (GGE): a Hilbert space Monte Carlo approach. [arXiv:1507.06994](https://arxiv.org/abs/1507.06994).
- [52] T. Langen, S. Erne, R. Geiger, B. Rauer, T. Schweigler, M. Kuhnert, W. Rohringer, I. E. Mazets, T. Gasenzer, and J. Schmiedmayer, Experimental observation of a generalized Gibbs ensemble, *Science* **348**, 207 (2015).
- [53] F. H. L. Essler, G. Mussardo, and M. Panfil, Generalized Gibbs ensembles for quantum field theories, *Phys. Rev. A* **91**, 051602 (2015);
F. H. L. Essler, G. Mussardo, and M. Panfil, On Truncated Generalized Gibbs Ensembles in the Ising Field Theory, *J. Stat. Mech.* (2017) 013103.
- [54] J. Cardy, Quantum quenches to a critical point in one dimension: some further results, *J. Stat. Mech.* (2016) 023103.
- [55] S. Sotiriadis, Memory-preserving equilibration after a quantum quench in a 1d critical model, *Phys. Rev. A* **94**, 031605 (2016).
- [56] A. Bastianello and S. Sotiriadis, Quasi locality of the GGE in interacting-to-free quenches in relativistic field theories, *J. Stat. Mech.* (2017) 023105.
- [57] E. Vernier and A. Cortés Cubero, Quasilocal charges and the complete GGE for field theories with non diagonal scattering, *J. Stat. Mech.* (2017) 23101.
- [58] B. Pozsgay, E. Vernier, and M. A. Werner, On Generalized Gibbs Ensembles with an infinite set of conserved charges, *J. Stat. Mech.* (2017) 093103.
- [59] T. Palmai and R. M. Konik, Quasi-local charges and the Generalized Gibbs Ensemble in the Lieb-Liniger model, [arXiv:1710.11289](https://arxiv.org/abs/1710.11289).
- [60] L. Vidmar and M. Rigol, Generalized Gibbs ensemble in integrable lattice models, *J. Stat. Mech.* (2016) 064007.
- [61] P. Calabrese and J. Cardy, Evolution of entanglement entropy in one-dimensional systems, *J. Stat. Mech.* (2005) P04010.
- [62] M. Fagotti and P. Calabrese, Evolution of entanglement entropy following a quantum quench: Analytic results for the XY chain in a transverse magnetic field, *Phys. Rev. A* **78**, 010306 (2008).
- [63] G. De Chiara, S. Montangero, P. Calabrese, and R. Fazio, Entanglement Entropy dynamics in Heisenberg chains, *J. Stat. Mech.* (2006) P03001.
- [64] V. Eisler and I. Peschel, Entanglement in a periodic quench, *Ann. Phys. (Berlin)* **17**, 410 (2008).
- [65] A. Laeuchli and C. Kollath, Spreading of correlations and entanglement after a quench in the Bose-Hubbard model, *J. Stat. Mech.* P05018 (2008).
- [66] H. Kim and D. A. Huse, Ballistic Spreading of Entanglement in a Diffusive Nonintegrable System, *Phys. Rev. Lett.* **111**, 127205 (2013).
- [67] M. G. Nezhadhighi and M. A. Rajabpour, Entanglement dynamics in short and long-range harmonic oscillators, *Phys. Rev. B* **90**, 205438 (2014).
- [68] A. Coser, E. Tonni, and P. Calabrese, Entanglement negativity after a global quantum quench, *J. Stat. Mech.* P12017 (2014).
- [69] M. Collura, P. Calabrese, and F. H. L. Essler, Quantum quench within the gapless phase of the spin-1/2 Heisenberg XXZ spin-chain, *Phys. Rev. B* **92**, 125131 (2015).
- [70] M. Fagotti and M. Collura, Universal prethermalization dynamics of entanglement entropies after a global quench, [arXiv:1507.02678](https://arxiv.org/abs/1507.02678).
- [71] P. Calabrese and J. Cardy, Quantum quenches in 1+1 dimensional conformal field theories, *J. Stat. Mech.* (2016) 064003.
- [72] J. S. Cotler, M. P. Hertzberg, M. Mezei, and M. T. Mueller, Entanglement Growth after a Global Quench in Free Scalar Field Theory, *JHEP* **11** (2016) 166.
- [73] A. S. Buyskikh, M. Fagotti, J. Schachenmayer, F. Essler, and A. J. Daley, Entanglement growth and correlation spreading with variable-range interactions in spin and fermionic tunnelling models, *Phys. Rev. A* **93**, 053620 (2016).
- [74] M. Kormos, M. Collura, G. Takács, and P. Calabrese, Real time confinement following a quantum quench to a non-integrable model, *Nature Physics* **13**, 246 (2017).
- [75] C. Pascu Moca, M. Kormos, and G. Zarand, Hybrid Semiclassical Theory of Quantum Quenches in One-Dimensional Systems, *Phys. Rev. Lett.* **119**, 100603 (2017).

- [76] M. Mestyan, B. Bertini, L. Piroli, and P. Calabrese, Exact solution for the quench dynamics of a nested integrable system, *J. Stat. Mech.* (2017) 083103.
- [77] C. von Keyserlingk, T. Rakovszky, F. Pollmann, and S. Sondhi, Operator hydrodynamics, OTOCs, and entanglement growth in systems without conservation laws, *Phys. Rev. X* **8**, 021013 (2018).
- [78] P. Calabrese, Entanglement and thermodynamics in non-equilibrium isolated quantum systems, *Physica A* **504**, 31 (2018).
- [79] I. Frerot, P. Naldesi, and T. Roscilde, Multi-speed prethermalization in spin models with power-law decaying interactions, *Phys. Rev. Lett.* **120**, 050401 (2018).
- [80] L. Hackl, E. Bianchi, R. Modak, and M. Rigol, Entanglement production in bosonic systems: Linear and logarithmic growth, *Phys. Rev. A* **97**, 032321 (2018).
- [81] E. Bianchi, L. Hackl, and N. Yokomizo, Linear growth of the entanglement entropy and the Kolmogorov-Sinai rate, *JHEP* (2018) 0325.
- [82] K. Najafi, M. A. Rajabpour, and J. Viti, Light-cone velocities after a global quench in a noninteracting model, *Phys. Rev. B* **97**, 205103 (2018)
- [83] B. Bertini, E. Tartaglia, and P. Calabrese, Entanglement and diagonal entropies after a quench with no pair structure, [arXiv:1802.10589](https://arxiv.org/abs/1802.10589).
- [84] J. Dubail, J.-M. Stéphan, J. Viti, P. Calabrese, Conformal field theory for inhomogeneous one-dimensional quantum systems: the example of non-interacting Fermi gases, *SciPost Phys.* **2**, 002 (2017).
- [85] M. Kormos and Z. Zimboras, Temperature driven quenches in the Ising model: appearance of negative Rényi mutual information, *J. Phys. A* **50** 264005 (2017).
- [86] V. Alba, Entanglement and quantum transport in integrable systems, [arXiv:1706.00020](https://arxiv.org/abs/1706.00020).
- [87] V. Eisler and D. Bauernfeind, Front dynamics and entanglement in the XXZ chain with a gradient *Phys. Rev. B* **96**, 174301 (2017).
- [88] M. Collura, M. Kormos, and G. Takacs, Dynamical manifestation of Gibbs paradox after a quantum quench, [arXiv:1801.05817](https://arxiv.org/abs/1801.05817).
- [89] X. Cao, A. Tilloy, and A. De Luca, Entanglement and transport of a fermion chain under continuous monitoring, [arXiv:1804.04638](https://arxiv.org/abs/1804.04638).
- [90] B. Bertini, M. Fagotti, L. Piroli, and P. Calabrese, Entanglement evolution and generalised hydrodynamics: noninteracting systems, [arXiv:1805.01884](https://arxiv.org/abs/1805.01884).
- [91] P. Calabrese and A. Lefevre, Entanglement spectrum in one dimensional systems, *Phys. Rev. A* **78**, 032329 (2008); V. Alba, P. Calabrese, and E. Tonni, Entanglement spectrum degeneracy and Cardy formula in 1+1 dimensional conformal field theories, *J. Phys. A* **51** 024001 (2018).
- [92] P. Calabrese and J. Cardy, Entanglement entropy and quantum field theory, *J. Stat. Mech.* P06002 (2004); P. Calabrese and J. Cardy, Entanglement entropy and conformal field theory, *J. Phys. A* **42**, 504005 (2009).
- [93] M. Caraglio and F. Gliozzi, Entanglement entropy and twist fields, *JHEP* 0811: 076 (2008); M. B. Hastings, I. Gonzalez, A. B. Kallin, and R. G. Melko, Measuring Renyi Entanglement Entropy with Quantum Monte Carlo, *Phys. Rev. Lett.* **104**, 157201 (2010).; C.-M. Chung, L. Bonnes, P. Chen, and A. M. Lauchli, Entanglement Spectroscopy using Quantum Monte Carlo, *Phys. Rev. B* **89**, 195147 (2014).
- [94] A. J. Daley, H. Pichler, J. Schachenmayer, and P. Zoller, Measuring Entanglement Growth in Quench Dynamics of Bosons in an Optical Lattice, *Phys. Rev. Lett.* **109**, 020505 (2012).
- [95] A. Elben, B. Vermersch, M. Dalmonte, J. I. Cirac, and P. Zoller, Renyi Entropies from Random Quenches in Atomic Hubbard and Spin Models, *Phys. Rev. Lett.* **120**, 050406 (2018).
- [96] R. Islam, R. Ma, P. M. Preiss, M. E. Tai, A. Lukin, M. Rispoli, and M. Greiner, Measuring entanglement entropy in a quantum many-body system, *Nature* **528**, 77 (2015).
- [97] V. Alba and P. Calabrese, Quench action and Rényi entropies in integrable systems, *Phys. Rev. B* **96**, 115421 (2017).
- [98] J.-S. Caux and F. H. L. Essler, Time evolution of local observables after quenching to an integrable model, *Phys. Rev. Lett.* **110**, 257203 (2013).
- [99] J.-S. Caux, The Quench Action, *J. Stat. Mech.* (2016) 064006.
- [100] V. Alba and P. Calabrese, Rényi entropies after releasing the Néel state in the XXZ spin-chain, *J. Stat. Mech.* **2017**, 113105 (2017).
- [101] L. Piroli, E. Vernier, and P. Calabrese, Exact steady states for quantum quenches in integrable Heisenberg spin chains, *Phys. Rev. B* **94**, 054313 (2016).
- [102] B. Pozsgay, Overlaps with arbitrary two-site states in the XXZ spin chain, *J. Stat. Mech.* (2018) 053103.
- [103] M. Takahashi, *Thermodynamics of one-dimensional solvable models*, Cambridge University Press, Cambridge, 1999.
- [104] E. Ilievski, M. Medenjak, T. Prosen, and L. Zadnik, Quasilocal charges in integrable lattice systems, *J. Stat. Mech.* (2016) P064008.
- [105] V. E. Korepin, N. M. Bogoliubov, and A. G. Izergin, *Quantum Inverse Scattering Method and Correlation Functions*, Cambridge University Press, 1993.
- [106] C. N. Yang and C. P. Yang, Thermodynamics of a One Dimensional System of Bosons with Repulsive Delta Function Interaction, *J. Math. Phys.* **10**, 1115 (1969).
- [107] B. Wouters, J. De Nardis, M. Brockmann, D. Fioretto, M. Rigol, and J.-S. Caux, Quenching the Anisotropic Heisenberg Chain: Exact Solution and Generalized Gibbs Ensemble Predictions, *Phys. Rev. Lett.* **113**, 117202 (2014); M. Brockmann, B. Wouters, D. Fioretto, J. D. Nardis, R. Vlijm, and J.-S. Caux, Quench action approach for releasing the Néel state into the spin-1/2 XXZ chain, *J. Stat. Mech.* (2014) P12009.

- [108] B. Pozsgay, M. Mestyán, M. A. Werner, M. Kormos, G. Zaránd, and G. Takács, Correlations after Quantum Quenches in the XXZ Spin Chain: Failure of the Generalized Gibbs Ensemble, *Phys. Rev. Lett.* **113**, 117203 (2014);
M. Mestyán, B. Pozsgay, G. Takács, and M. A. Werner, Quenching the XXZ spin chain: quench action approach versus generalized Gibbs ensemble, *J. Stat. Mech.* (2015) P04001.
- [109] V. Alba, and P. Calabrese, The quench action approach in finite integrable spin chains, *J. Stat. Mech.* (2016), 043105.
- [110] A. Faribault, P. Calabrese, and J.-S. Caux, Quantum quenches from integrability: the fermionic pairing model, *J. Stat. Mech.* P03018 (2009);
A. Faribault, P. Calabrese, and J.-S. Caux, Bethe ansatz approach to quench dynamics in the Richardson model, *J. Math. Phys.* **50**, 095212 (2009).
- [111] V. Gritsev, T. Rostunov, and E. Demler, Exact methods in the analysis of the non-equilibrium dynamics of integrable models: application to the study of correlation functions for non-equilibrium 1D Bose gas, *J. Stat. Mech.* (2010) P05012.
- [112] B. Pozsgay, Overlaps between eigenstates of the XXZ spin-1/2 chain and a class of simple product states, *J. Stat. Mech.* (2014) P06011.
- [113] P. Le Doussal and P. Calabrese, The KPZ equation with flat initial condition and the directed polymer with one free end *J. Stat. Mech.* (2012) P06001;
P. Calabrese and P. Le Doussal, Interaction quench in a Lieb-Liniger model and the KPZ equation with flat initial conditions *J. Stat. Mech.* (2014) P05004.
- [114] J. De Nardis, B. Wouters, M. Brockmann, and J.-S. Caux, Solution for an interaction quench in the Lieb-Liniger Bose gas, *Phys. Rev. A* **89**, 033601 (2014).
- [115] M. Brockmann, J. D. Nardis, B. Wouters, and J.-S. Caux, A Gaudin-like determinant for overlaps of Néel and XXZ Bethe states, *J. Phys. A* **47**, 145003 (2014);
M. Brockmann, Overlaps of q-raised Néel states with XXZ Bethe states and their relation to the Lieb-Liniger Bose gas, *J. Stat. Mech.* (2014) P05006;
M. Brockmann, J. De Nardis, B. Wouters, and J.-S. Caux, Néel- XXZ state overlaps: odd particle numbers and Lieb-Liniger scaling limit, *J. Phys. A* **47**, 345003 (2014).
- [116] L. Piroli and P. Calabrese, Recursive formulas for the overlaps between Bethe states and product states in XXZ Heisenberg chains, *J. Phys. A* **47**, 385003 (2014).
- [117] M. de Leeuw, C. Kristjansen, and K. Zarembo, One-point functions in defect CFT and integrability, *JHEP* **08** (2015) 098;
I. Buhl-Mortensen, M. de Leeuw, C. Kristjansen, and K. Zarembo, One-point Functions in AdS/dCFT from Matrix Product States, *JHEP* **02** (2016) 052;
O. Foda and K. Zarembo, Overlaps of partial Néel states and Bethe states, *J. Stat. Mech.* (2016) 23107.
- [118] M. de Leeuw, C. Kristjansen, and S. Mori, AdS/dCFT one-point functions of the $SU(3)$ sector, *Phys. Lett. B* **763**, 197 (2016).
- [119] B. Pozsgay and V. Eisler, Real-time dynamics in a strongly interacting bosonic hopping model: Global quenches and mapping to the XX chain, *J. Stat. Mech.* (2016) 053107.
- [120] D. X. Horváth, S. Sotiriadis, and G. Takács, Initial states in integrable quantum field theory quenches from an integral equation hierarchy, *Nucl. Phys. B* **902**, 508 (2016);
D. X. Horváth and G. Takács, Overlaps after quantum quenches in the sine-Gordon model, *Phys. Lett. B* **771**, 539 (2017).
- [121] P. P. Mazza, J.-M. Stéphan, E. Canovi, V. Alba, M. Brockmann, and M. Haque, Overlap distributions for quantum quenches in the anisotropic Heisenberg chain, *J. Stat. Mech.* (2016) 013104.
- [122] B. Bertini, D. Schuricht, and F. H. L. Essler, Quantum quench in the sine-Gordon model, *J. Stat. Mech.* (2014) P10035.
- [123] B. Bertini, L. Piroli, and P. Calabrese, Quantum quenches in the sinh-Gordon model: steady state and one-point correlation functions, *J. Stat. Mech.* (2016) 063102.
- [124] B. Bertini, E. Tartaglia, and P. Calabrese, Quantum Quench in the Infinitely Repulsive Hubbard Model: the Stationary State, *J. Stat. Mech.* **2017**, 103107 (2017).
- [125] L. Piroli, P. Calabrese, and F. H. L. Essler, Multiparticle Bound-State Formation following a Quantum Quench to the One-Dimensional Bose Gas with Attractive Interactions, *Phys. Rev. Lett.* **116**, 070408 (2016);
L. Piroli, P. Calabrese, and F. H. L. Essler, Quantum quenches to the attractive one-dimensional Bose gas: exact results, *SciPost Phys.* **1**, 001 (2016).
- [126] L. Piroli, B. Pozsgay, and E. Vernier, What is an integrable quench?, *Nucl. Phys. B* **925**, 362 (2017).
- [127] G. Delfino, Quantum quenches with integrable pre-quench dynamics, *J. Phys. A* **47** (2014) 402001.
- [128] S. R. White and A. E. Feiguin, Real-Time Evolution Using the Density Matrix Renormalization Group, *Phys. Rev. Lett.* **93**, 076401 (2004).
- [129] A. J. Daley, C. Kollath, U. Schollock, and G. Vidal, Time-dependent density-matrix renormalization-group using adaptive effective Hilbert spaces, *J. Stat. Mech.* (2004) P04005.
- [130] U. Schollwöck, The density-matrix renormalization group, *Rev. Mod. Phys.* **77**, 259 (2005).
- [131] U. Schollwöck, The density-matrix renormalization group in the age of matrix product states, *Annals of Physics* **326**, 96 (2011).
- [132] For the implementation we used the ITENSOR library (<http://itensor.org/>).
- [133] V. Alba, Towards a Generalized Hydrodynamics description of Rényi entropies in integrable systems, [arXiv:1807.01800](https://arxiv.org/abs/1807.01800).
- [134] L. Bonnes, F. H. L. Essler, and A. M. Läuchli, “Light-cone” dynamics after quantum quenches in spin chains, *Phys. Rev. Lett.* **113**, 187203 (2014).